

QATAR UNIVERSITY

COLLEGE OF ENGINEERING

DESIGN OF REAL-TIME FUZZY LOGIC PSS BASED ON PMUs FOR DAMPING
LOW FREQUENCY OSCILLATIONS

BY

JAMIL UR RAHMAN MAHMOOD UR REHMAN

A Thesis Submitted to the Faculty of

College of Engineering

in Partial Fulfillment

of the Requirements

for the Degree of

Master of Science in

Electrical Engineering

June 2016

© 2016 Jamil ur rahman Mahmood ur Rehman. All Rights Reserved.

The members of the Committee approve the thesis of **Jamil ur rahman Mahmood ur Rehman** defended on 17 May 2016.

Dr. Khaled Ellithy

Thesis/Dissertation Supervisor

Dr. Khaled El-Metwally

Committee Member

Dr. Nader Meskin

Committee Member

Dr. Hasan Mehrjerdi

Committee Member

Approved:

Dr. Khalifa Nasser Al-Khalifa, Dean, College of Engineering

Abstract

Poorly damped low frequency oscillations is one of the main problems threatening safe and stable operation of the interconnected power systems and reducing the capability of transmission the power. The generator's excitation system has been supplemented with the Power System Stabilizer (PSS) in order to improve the damping of these low oscillations. In the latest smart power grids, the Phasor Measurement Units (PMUs) become a fundamental element in the monitoring, protection and control applications as PMU signals are more accurate than the conventional measurement units and real time GPS stamped. In this study, Fuzzy Power System Stabilizer (FPSS) has been designed and its performance in damping inter-area oscillations compared with the conventional PSS (CPSS) based on the simulation with MATLAB/Simulink model. The results of the simulation with the Simulink model proved that the performance of the designed FPSS in damping inter-area oscillation is better than the CPSS. One of the main features of fuzzy controller is that it doesn't require mathematical modeling as it is designed based on the time-domain and the operator experience while, in contrast, the conventional PSS requires to be designed in the frequency domain. Real Time Digital Simulator (RTDS) has been used to develop the real-time models of the test systems. The time-domain simulations with the RTDS model when the system subjected to the large disturbance (three-phase to ground fault) have been performed to show that the designed FPSS improved the damping of the oscillations effectively. The simulation results have been verified by modal analysis.

Table of Contents

List of Figures	ix
List of Tables	xii
Acronyms	xiii
Notations	xiv
Acknowledgment	xvi
Chapter 1: Introduction	1
1.1 Objective and Motivation	2
1.2 Power System Stability	3
1.2.1 Steady State Stability	3
1.2.2 Transient Stability	4
1.3 Types of Oscillations	5
1.3.1 Inter-area Oscillation Modes	5
1.4 Interconnecting Electric Power Grids	6
1.5 Fuzzy Logic	6
1.5.1 Fuzzy Logic Applications in Engineering	7
1.6 Phasor Measurement Unit (PMU)	7
1.7 Real Time Digital Simulator (RTDS)	9
1.8 Excitation System	10
1.8.1 Exciter	11

1.8.2	Power System Stabilizer	12
1.9	Electrical System Fault.....	12
1.9.1	Transient Fault	13
1.9.2	Persistent Fault.....	14
1.9.3	Symmetrical (Balanced) Fault	14
1.9.4	Unsymmetrical (Unbalanced) Fault	14
1.10	Fault-Clearing Time	14
Chapter 2: Literature Review.....		16
2.1	Control Methods to Enhance the Damping of the LFOs.....	16
2.2	Input Signals to FPSS.....	18
2.3	Linguistic Control Variables	19
2.4	Membership Function	19
2.5	Measurement device of PSS inputs.....	21
2.6	Summary of the Literature Review	22
2.7	Contributions of the Thesis	25
Chapter 3: Power System Modeling and Methods of Analysis		26
3.1	Synchronous Generator Modeling	26
3.1.1	Four Winding Model (6 th Order Model).....	28
3.1.2	Two-Axis Model (4 th Order Model)	29
3.1.3	One-Axis Model (3 rd Order Model).....	30

3.1.4	Classical Model (2 nd Order)	30
3.2	Turbine-Governor Model	32
3.3	Modeling of the Exciter.....	33
3.4	PSS Modeling.....	34
3.5	Transmission Line Models	35
3.6	Load Model	37
3.7	Linearization of the Power System Model.....	38
3.7.1	Generator linearization.....	38
3.7.2	Exciter Model Linearization	40
3.7.3	Linearization of PSS	40
3.8	Modal Analysis	41
3.8.1	Assessment of the Stability Using Modal Analysis.....	42
Chapter 4: FPSS Design Based on PMU Signals		45
4.1	State and Control Variables.....	45
4.2	Fuzzification.....	47
4.3	Rule-Base Design.....	47
4.4	Inputs and output Membership Functions.....	50
4.5	De-Fuzzification.....	52
4.6	Output Signal.....	53
4.7	FPSS in MATLAB/Simulink	53

4.8	Practical Implementation of the FPSS	55
Chapter 5: MATLAB/Simulink Simulation.....		57
5.1	Two-Area Power System	57
5.2.1	System Behavior without PSS.....	59
5.3.1	System Behavior with PSS	62
5.4.1	System Behavior with Increase in the Load	68
5.2	Summary of the Simulation.....	71
Chapter 6: Implementation and Experimental Results		73
6.1	Implementation on SMIB.....	73
6.2	Implementation on Two-Area Power System	76
6.2.1	Time Response with Fault:	77
6.2.2	Best Location for Single FPSS	80
Chapter 7: Conclusion and Future Work		87
7.1	Conclusion.....	87
7.2	Future Work	88
References.....		90
Appendix A: Papers and Posters.....		99
Appendix B: RTDS Model		100
Appendix C: MATLAB Code used for FPSS.....		101
Appendix D: MATLAB code for Finding Eigenvalues.....		102

Appendix E: ARM μ -Controller Code.....	103
---	-----

List of Figures

Figure 1: Power system stability categories.....	3
Figure 2: PMU Connection [14]	9
Figure 3: Types of the electrical fault	13
Figure 4: Different types of membership functions	20
Figure 5: Schematic diagram of the synchronous machines.....	27
Figure 6: Governor model.....	32
Figure 7: IEEE Type AC4A Excitation System Model	34
Figure 8: General block diagram of the conventional PSS.....	35
Figure 9: Medium transmission line representation, nominal π configuration	36
Figure 10: Medium transmission line representation, nominal T configuration	37
Figure 11: IEEE Type AC4A Excitation System Model	40
Figure 12: FPSS block diagram	46
Figure 13: Response of the power transmitted between the areas in the two-area power system and the output signal of the FPSS (V_s).....	48
Figure 14: Membership function of the inputs/output normalized from -1 to1	51
Figure 15: FPSS block diagram in MATLAB/Simulink	53
Figure 16: Inputs and output membership function	54
Figure 17: Rules that relate inputs to the outputs	55
Figure 18: ARM μ -controller.....	56
Figure 19: One-line diagram of the 4-machine 2-area power test system with PMU in each area.....	58
Figure 20: Simulink model of the two-area power system	59

Figure 21: Response of the power exported from area 1 to area 2 without PSS	60
Figure 22: Response of voltage at bus 8 without PSS	61
Figure 23: Response of the rotor speed for the four generators without PSS.....	62
Figure 24: Response of the power exported from area 1 to area 2	63
Figure 25: Response of voltage at bus 8 for a fault of 0.200 sec.....	64
Figure 26: Response of the rotor speed of the four generators in presence of the designed FPSS	65
Figure 27: Response of the rotor speed of the four generators in presence of the CPSS	66
Figure 28: Response of the rotor speed of generator 1 and generator 2	67
Figure 29: Response of the power exported from area 1 to area 2 with increase in the load by 5% in area 2.....	68
Figure 30: Response of the power exported from area 1 to area 2 with increase in the load by 10% in area 2.....	69
Figure 31: Response of the power exported from area 1 to area 2 with increase in the load by 20% in area 2.....	70
Figure 32: Response of the power transmitted from Area 1 to Area 2 [59].	72
Figure 33: Experimental Setup	73
Figure 34: SMIB power system	74
Figure 35: Response of generator speed of SMIB	75
Figure 36: Response of generator output power of SMIB.....	75
Figure 37: One-line diagram of the 4-machine 2-area power test system with PMU in each area.....	77
Figure 38: Response of voltage at the faulted bus	78

Figure 39: Response of the power exported to area 2 from area 1	79
Figure 40: Response of the rotor speed for the four generators with FPSS with all generators	80
Figure 41: Response of the power exported to area 2 from area 1 with FPSS at area 1 only	81
Figure 42: Response of the power exported to area 2 from area 1 with FPSS at area 2 only	81
Figure 43: Response of the rotor speed for the four generators with FPSS in Area 1 only	82
Figure 44: Response of the rotor speed for the four generators with FPSS in Area 2 only	82
Figure 45: Response of the power exported to area 2 from area 1 with FPSS on Generator 3 only.	83
Figure 46: Response of the power exported to area 2 from area 1 with FPSS on Generator 4 only.	84
Figure 47: Response of the rotor speed for the four generators with FPSS with generator 3 only	84
Figure 48: Response of the rotor speed for the four generators with FPSS with generator 4 only	85
Figure 49: GCC Interconnected Power Grid [14].....	88
Figure 50: Two-area power system model in RTDS	100

List of Tables

Table 1: Comparison between SCADA and PMUs [61]	22
Table 2: Literature review summary	23
Table 3: Summary of states in each model	31
Table 4: Eigenvalue and system stability.....	44
Table 5: Raw rule-base for FPSS	49
Table 6: Final rule-base for FPSS	50
Table 7: Falling and Rising Sides of the membership function.....	52
Table 8: Eigenvalues associated with electro-mechanical oscillation mode	76
Table 9: Eigenvalues associated with inter-area oscillation mode	86
Table 10: MATLAB code for inserting FIS file in Fuzzy Logic Controller.....	101
Table 11: MATLAB code for Finding Eigenvalues.....	102
Table 12: C code for programming FPSS on μ -Controller	103

Acronyms

CPSS Conventional Power System Stabilizer

FPSS Fuzzy Logic Power System Stabilizer

AVR Automatic Voltage Regulator

PSS Power System Stabilizer

RTDS Real Time Digital Simulator

LFOs Low Frequency Oscillations

FLC Fuzzy Logic Controller

Notations

δ	Rotor angle of Synchronous Generator [rad]
ω	Frequency of oscillations [rad/sec]
ω_s	Synchronous rotor speed [rad/sec]
T_m	Mechanical torque [pu]
$\Delta\omega$	Frequency deviation
P_e	Electrical output power [pu]
E_{fd}	Excitation field voltage [pu]
T_e	Electric torque [pu]
$E'_{d,q}$	Internal voltage behind the transient reactance [pu]
$X_{d,q}$	Steady state reactance of d-/q-axis [pu]
$X'_{d,q}$	Transient reactance of d-/q-axis [pu]
$X''_{d,q}$	Sub transient reactance of d-/q-axis [pu]
$I_{d,q}$	Current in d-/q-axis
T_{FW}	Torque represents friction and windage losses [pu]
H	Inertia constant

$T'_{d0,q0}$	Transient time constant of excitation circuit, d-/q-axis [sec]
$T''_{d0,q0}$	Sub transient time constant of excitation circuit, d-/q-axis [sec]
X_{ls}	Armature leakage reactance
ψ_{1d}	Flux linkage of the damper winding, d-axis
ψ_{2q}	Flux linkage of the damper winding, q-axis
K_{PSS}	Power system stabilizer gain

Acknowledgment

All thanks and praise is to Allah for his help. I'm so grateful to my supervisor Dr. Khaled for his instructing, insightful comments and suggestions. I also would like to thank the College of Engineering at Qatar University as this study was supported by it. Furthermore, I want to express thanks to my colleague Sami who helped me a lot in programming the Microcontroller.

Words are not enough when it comes to thanking my family, as they continuously supported me and selflessly endured my absence throughout the study. I am very grateful to them.

Chapter 1: Introduction

Globally, the power demand is growing rapidly which makes the power systems almost reach to their limits. This issue introduces poorly damped or unstable low frequency oscillation, especially through weak long tie lines [1]. If these oscillations occurred between adjacent synchronous generators on the same power generation area, they are called local area oscillations. If they are occurred between the generators in different areas, they are called inter area oscillations. To enhance the damping of these oscillations and hence improve the stability of the power systems, a component known as Power System Stabilizer (PSS) is added to the generator's excitation system.

In this thesis, a Fuzzy Logic based Power System Stabilizer (FPSS) for damping the low frequency oscillations has been designed using unity triangular membership functions for both of the input and output variables. This thesis is structured as follows: Chapter 1 sheds light on the theoretical background, while Chapter 2 introduces the literature review. The power system modelling is presented in Chapter 3 as well as the linearization of the power system. The details of designing the FPSS are presented in Chapter 4. In Chapter 5, the designed FPSS has been tested on the two-area power system based on simulation with MATLAB/Simulink model and the performance of it has been compared with the conventional PSS. Then, the experimental results for Single Machine Infinite Bus (SMIB) system and 2-area power system are provided in Chapter 6. Finally, in the last chapter, the conclusion as well as the future works are reported.

1.1 Objective and Motivation

The aims of the research reported in this thesis are:

1. To design a fuzzy based PSS to enhance both dynamic and transient stability.
2. To implement the designed FPSS in real-time using RTDS based on the global signals obtained from the PMUs.
3. To improve the quality of the transferred power between two interconnected power grids.
4. To highlight the advantages of using FPSS as an alternative to the conventional PSS.

This research has many areas in which it can be beneficial such as:

1. To improve the damping of inter-area oscillations mode due to the weak-ties in the Gulf Cooperation Council (GCC) grid.
2. To encourage the development of equipment based on fuzzy logic principles for power generation.
3. To realize Qatar vision 2030 by changing the current power grid to the smart one which is monitored by wide area monitoring systems based on Phasor Measurement Unit.

1.2 Power System Stability

Power system stability describes the ability of a synchronous power system, for a given initial operating condition, to return to stable condition, steady state, after being subjected to a quite large disturbance due to large step loading or loss of generation etc., so the entire system remains intact [2].

Power system stability categories are shown in Figure 1 which followed by a brief description of each category:

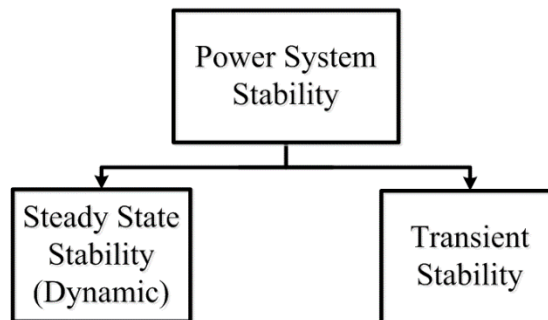


Figure 1: Power system stability categories

1.2.1 *Steady State Stability*

The Steady State Stability describes the ability of the power system to bring itself back to its stable configuration following small and gradual changes in the

network (small change in the load, change in solar PV output and small generator tripping). It is also called dynamic stability [3].

In this analysis, it should be checked that the bus voltages are kept close to their nominal values, the phase angles between two buses are not too large and the power equipment and transmission lines are not overloaded [3].

If the power flow in the system is about to exceed the maximum allowable ranges after which it is possible that one or more of the connected generators will lose their synchronism, then, it is said that the steady state stability limits have been reached [3].

1.2.2 Transient Stability

The Transient Stability describes the ability of the power system to bring itself back to its stable condition after a large disturbance occurred for a short period of time such as transmission line and large generator trips [3].

In this analysis, it should be checked that the load angle returns to a steady value when the fault or the disturbance has been cleared [3].

When reaching the maximum allowable power flow in the system without causing any instability to the system after a large disturbance, it is said that the system reached its transient stability limits. Any further disturbance beyond that will cause the system to become unstable [3].

1.3 Types of Oscillations

The main electromechanical oscillations caused by the disturbances in the power systems can be categorized as the following:

1. Local modes: These oscillations are occurred between a single generator and the rest of the generating unit as well as between the generating unit and the rest of the power system. The typical range of these oscillations is 1 Hz-2 Hz [4].
2. Intra-plant modes: These oscillations are occurred between the generators in the same generating plant and their range is 2 Hz-3 Hz [4].
3. Inter-area modes: These oscillations are occurred when a group of generators in a specific area oscillate together against another group of generators in a different area. These oscillations are on type of the low frequency oscillations and the typical range of them is 0.1 Hz-0.8 Hz [3].

1.3.1 Inter-area Oscillation Modes

The inter-area oscillations are type of low-frequency electromechanical oscillations (LFEOs) and as mentioned above, are occurred when a group of generators in a specific area swings against another group of generators in a different area. The main causes of these oscillations are the high gain of the exciters or when a high power transferred through the weak long tie lines. The inter-area

oscillations should be damped immediately as they will risk the secure operations of the power system. They can even cause a power system blackout [5].

1.4 Interconnecting Electric Power Grids

Interconnecting the electric power grids of different countries provide many benefits that can be summarized in security and reliability. It reduces the operating cost as the need for the standby capacity to meet fluctuations in the demand will be reduced as at the peak times, the required electricity will be imported from cheap foreign generators, while during the low demand, it will be exported. It will also help in locating new generating plants close to the sources of inexpensive fuel [6]. Additionally, the overall level of environmental pollution will be reduced. The Gulf Cooperation Council (GCC) interconnection is an example of interconnecting the power grids.

However, this interconnection of power grids is subject to low frequency inter-area oscillations which are caused by transmitting a large amount of power through the weak tie lines, which means that the possibility of a blackout in the GCC exists because of those oscillations.

1.5 Fuzzy Logic

The concept of fuzzy logic was proposed by Zadeh in 1965 and was used in many applications in different areas. It is a method for computing based on “degrees of truth” instead of the usual “totally true”/“totally false”, 1 or 0, Boolean logic on which the modern computers have been built. Fuzzy logic includes a range of partial

truth from “almost certain” to “very unlikely” (gray areas of probability) [7], so that, for instance, it can be said that the statement, today is sunny, is 0% true if it is heavily overcast, 50% true if it's hazy, 75% true if only a few clouds are shown in the sky, and 100% true if there are no clouds at all.

Human language cannot be translated easily into the absolute terms of the regular Boolean logic, 0 and 1. Fuzzy logic works on the manner closer to the way on which the human kind brains work. Human kind brain collects data from the surrounding environment and forms a number of partial truths which it gathers further toward higher truths that, again, when certain thresholds are exceeded, cause other results such as the reaction of the motor. A similar process is used in the artificial computer neural network and expert systems [8].

1.5.1 Fuzzy Logic Applications in Engineering

There are many applications for fuzzy logic in the different aspects of the life. For instance, it is used to design a fuzzy PSS, as in this thesis, robots and control their motion. It is also used in designing the controllers such as PI, PD, PID. Furthermore, it is used in designing the self-tuning controllers where the fuzzy systems and neural networks have been combined together to enhance the performance of the fuzzy controllers [9].

1.6 Phasor Measurement Unit (PMU)

In the latest smart power grids, Phasor Measurement Unit (PMU) is considered as the most important measurement devices. The first PMU was

developed at Virginia Tech University by Dr. Arun G. Phadke and Dr. James S. Thorp in 1988 [12]. However, the first commercial PMU saw the light in 1992 by Macrodyne [13]. PMU technology continuously developed throughout the 1990's, mostly because of the evolution in wireless communication technology and digital control.

There are many applications and functions for PMUs in the smart power grids such as controlling, monitoring and protection. Power system monitoring is the key application of PMUs which can be seen obviously in monitoring wide-area disturbances, either the inter-area mode of oscillations or the local mode of oscillations (low frequency electro-mechanical oscillations). PMUs are expected to be the essential element in the next generations of wide area monitoring systems (WAMS) which have a great potential in many applications related to the power systems, including the monitoring of the power oscillation and power damping. In Figure 2, it can be noticed that the synchronized phasors of the current as well as the voltage can be obtained from the PMU in addition to the measurements of the frequency and the rate on which the frequency changes. The Global Positioning System satellite (GPS) clock is used in synchronization the sampling of the voltage and current waveforms at the same time.

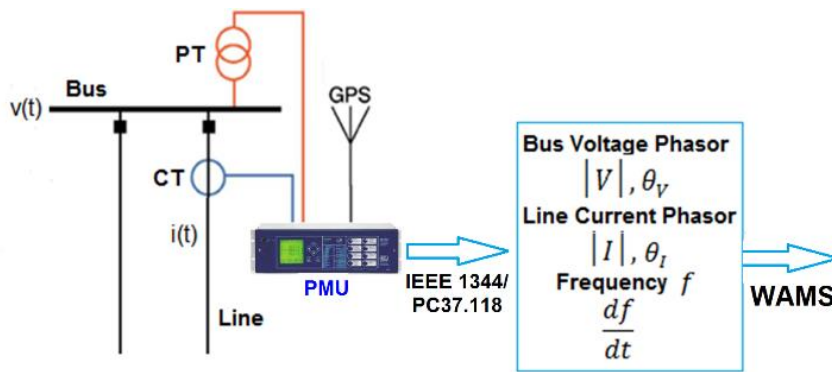


Figure 2: PMU Connection [14]

Since one of the objectives of the research reported in this thesis is to increase the ability of the interconnected power grids to damp the inter-area oscillations using the global signals which are obtained from the PMUs, so this method has many benefits when used in the GCC countries smart power grid in the future [14]. The GCC grid is expected to face the problem of unstable and/or poor damping of inter-area oscillations mode due to the weak-ties in the grid. These unstable modes could lead the grid to blackout.

1.7 Real Time Digital Simulator (RTDS)

Real Time Digital Simulator (RTDS) is the world's reference for executing real time simulations as it has capability to do the simulation in a time close to real time for actual events. It is used in transient phenomena to obtain precise and accurate modeling and analysis where it is very dangerous and costly to test the controller on real live system for the sake of emulating rare faults or danger situation. RTDS can be used instead to deliver a controlled and safe environment

to simulate and implement the faults. The overall system performance can be enhanced through the closed-loop testing circumstances that is so closed to the real environment conditions. The first application of real-time power system monitoring arisen in late eighties, utilizing the power measurement unit [13].

In this thesis, the RTDS has been used in developing and testing the designed real-time FPSS. As the PMUs needs to be fed by the measured voltages and currents of the system as analog signals, RTDS will provide these signals.

1.8 Excitation System

The synchronous generator requires DC electric power supplied to the field windings in the rotor which produces a magnetic flux in order to induce the AC voltage and current in the stator armature. That DC current can be supplemented by the excitation system which also controls the generator terminal voltage. The required amount of excitation to keep the output voltage equals to the nominal value can be determined by the connected load. If the load increases, the required amount of excitation increases [15].

The excitation system consists of the following elements:

1. Exciter: It is the DC power source of the field winding of the generator.
2. Terminal voltage transducer: It measures the generator terminal voltage, converts it to the DC voltage which will be compared with a reference voltage.

3. Automatic Voltage Regulator (AVR): It amplifies the error signal obtained from the voltage transducer to the appropriate level and form which used as the input control signals for the exciter.
4. Power system stabilizer: Its output can be used as input signal to the AVR to damp the power system oscillations through the excitation system.
5. Limiters and protective circuit: It prevents exceeding the limits of the exciter and generator.

1.8.1 Exciter

The exciter can be either separate from the generator, separately-excited, or combined with the generator, self-excited. Separately-excited type is usually a DC generator that is run either by an AC motor or by a small steam turbine. The self-excited type gets the required power from the generator itself which can be static systems or run by turbine-generator shaft. In static excitation systems, all components are static or stationary which represented in the form of static rectifiers and the required power for excitation is supplied from the generator terminals directly after stepping down the voltage to certain level by a transformer or the power can be taken from the auxiliary windings of the generator [16]. In the excitation system run by the shaft, power is generated by a small AC or DC generator which is run by the same main shaft of the unit.

1.8.2 Power System Stabilizer

Under steady-state conditions, automatic voltage regulator (AVR) helps in enhancing the stability of the power system, but it is not enough to keep the system stable during the transient conditions especially when power systems are interconnected where high loading may occur on the interconnection lines [17]. To overcome this problem, the AVR control loop has been supplemented by the power system stabilizer, PSS [18]. Enhancing both dynamic and transient stability is the rule of the PSS by supplying an electrical torque (that is in phase with the rotor speed deviation) to the synchronous machine rotor through the excitation system to add positive damping to the rotor's oscillations [16].

However, this CPSS has some limitations which are covered in Chapter 2 that can be overcome with the fuzzy logic based PSS (FPSS). The details of the FPSS are mentioned in Chapter 4.

1.9 Electrical System Fault

It is abnormal condition that interferes with the normal system operations due to failure of the electrical components in the system such as transmission lines, transformers and generators.

It can cause over current flow in the circuit. In such case, a heavy current being drawn from the source which damages insulation and components of the equipment and causes tripping of relays and even may cause electrical fires. It also can kill the human or cause severe injuries.

The types of the fault in the power system illustrated in Figure 4 which followed by a brief description of each type.

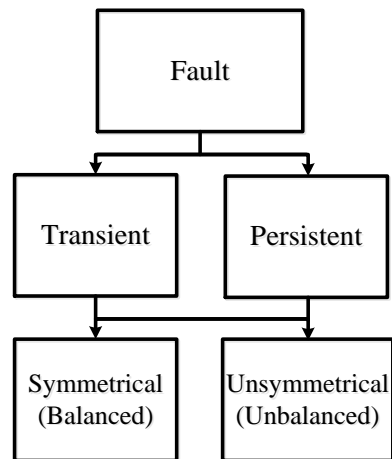


Figure 3: Types of the electrical fault

1.9.1 Transient Fault

This fault is cleared when the power system protection isolates area of the fault for a short period such as momentary contacting of the transmission line to a tree or lightning strike.

1.9.2 Persistent Fault

This fault cannot be cleared even the power system protection isolated area of the fault as happening with the underground cables contact because of the mechanical damage.

On the other hand, electrical fault can be either symmetrical or unsymmetrical. The brief description given below for each type.

1.9.3 Symmetrical (Balanced) Fault

In this type, the three phases are affected equally. This fault is rare but very dangerous. It can be either three-phase to ground (L-L-L-G) or line to line to line (L-L-L) faults.

1.9.4 Unsymmetrical (Unbalanced) Fault

In this type, the three phases are affected unequally. It can be line to ground (L-G), line to line (L-L) as well as double line to ground (LL-G) faults.

1.10 Fault-Clearing Time

When a fault occurred in the grid, the faulty element should be isolated from the grid. That function can be done using a circuit breaker. The time interval required to clear the fault starting from the time of occurrence is called the fault-clearing time. Practically, the shortest possible fault-clearing time is preferable to avoid any further damage for the grid elements [19]. The critical clearing time (CCT) can be defined as the maximum time during which the system remains

transiently stable [20]. The CCT range for the high voltage (HV) transmission systems is 30-70 milliseconds [21].

Chapter 2: Literature Review

There are many studies have been published in the field of damping the low frequency oscillations. In this chapter, some aspects related to the control methods of damping low frequency oscillations (LFOs), comparison between the CPSS and FPSS and the parameters related to the design of the FPSS are covered.

2.1 Control Methods to Enhance the Damping of the LFOs

De-Mello and Concordia perhaps are the first researcher who pointed out that the absence of the damping torque is due to AVR action that causes the low frequency oscillations [55]. They proposed to add a supplementary control loop known as the PSS to reduce that negative damping. For that reason, they designed a PSS using the speed signal as input and showed the effect of it through time domain simulations.

However, that conventional PSS uses lead-lag compensation and the parameters of it are fixed and obtained using linearized power system model (its design neglects the non-linearity of the power systems) for a specific operating point around which the performance of it is very good. This results into poor performance in practical non-linear power systems under different operating points where it may not be effective as the parameters of the stabilizer are fixed [22].

Many control methods have been proposed to overcome that problem and enhance the damping characteristic of the low frequency oscillations. Alkhatib proposed a dynamic genetic algorithms to be used for robust design of multi-

machine power system stabilizers [23]. Mostafa used Particle Swarm Optimization (PSO) for designing Power System Stabilizers [24]. Ellithy realizing the system stabilizers using μ -Controller based on damping torque technique [25]. Bevrani has used the PID in his design [26]. Segal has used artificial neural network to make a self-tuning power system stabilizer [27]. Sumina used Eigen value sensitivity for parameter tuning of power system stabilizer [28].

Among of these controllers is the fuzzy logic PSS that can be designed to stabilize the power system by improving the damping of these low frequency oscillations [29].

In contrast with CPSS, fuzzy logic based PSS performs more efficiently than CPSS in varying environment for different operating points as it is fed by the measured values of the plant output from which it determines the operating condition and compares it with the rule-base. Based on comparison, it applies the appropriate required control actions [30].

One of the main features of fuzzy controller is that it doesn't require any complex mathematical modeling as it is designed based on in the time domain and the operator experience while, in contrast, the conventional one is designed in frequency domain [31].

Unfortunately, since the power systems are so non-linear and so sophisticated, this causes the design of the rule-base of the FPSS to become difficult and need the expert knowledge or offline simulation [56].

There are also research in which fuzzy logic combined with other methods. For instance, in his paper, You and Gholipour combined fuzzy logic method with neural networks to get new method which is adaptive neuro-fuzzy inference-system (ANFIS) [32] [60].

2.2 Input Signals to FPSS

To design a fuzzy logic based PSS, the first step is to select the state variables that represent the system dynamic performance which will be considered as the input signals to the fuzzy logic controller. Usually in general, FPSS is a two-input and a single-output system. However, many researchers proposed to use the change of rotor speed ($\Delta\omega$) and the rate of change of the rotor speed ($\Delta\dot{\omega}$) as the inputs as Gupta and Shah did [31] [33]. Ul Banna proposed to use the tie-line active power deviation (ΔP) as input signal in conjunction with the rotor speed deviation [30]. Soliman used three inputs in his paper which are the tie-line reactance (X_e), reactive power (Q) and active power (P) [34].

In this study, the system frequency deviation and its differentiation have been chosen to be the input signals to the FPSS because the consideration of frequency deviation has some advantages as the grid frequency value is independent of the system configuration and operating procedures and it is considered as universally acceptable stabilizing signal [35]. Also, there is a relationship between the system frequency and the consumed power as the system frequency will vary as the consumed power changes.

2.3 Linguistic Control Variables

The number of the required linguistic variables that are used in converting the inputs to the fuzzy set depends on the application but as a general trend, it is an odd number [33]. In his paper, Umrao used five linguistic variables to describe the input and output [36], so the number of rules was 25. Ul Banna used seven linguistic variables in his comparison between CPSS and FPSS which led to 49 rules [30]. However, if the total number of the linguistic variables is increased, the precision of control will be enhanced. On the other hand, the computational time will be increased as well as the required memory because of the increasing of number of linguistic variables.

It can be inferred from the literature review that seven linguistic variables are reasonably enough, so the number of the linguistic variables used in this study is seven rules which leads to 49 rules.

2.4 Membership Function

A membership function can be defined as a curve that describes how to map the non-fuzzy numeric input data into the linguistic variable terms by mapping each value in the input space to a membership value (or degree of membership) between 0 and 1 [10].

The shapes of the membership functions are important for a particular problem since they affect on a fuzzy inference system. The shape of the membership

functions may be triangular, trapezoidal, Gaussian and sigmoidal [11] as shown in Figure 4.

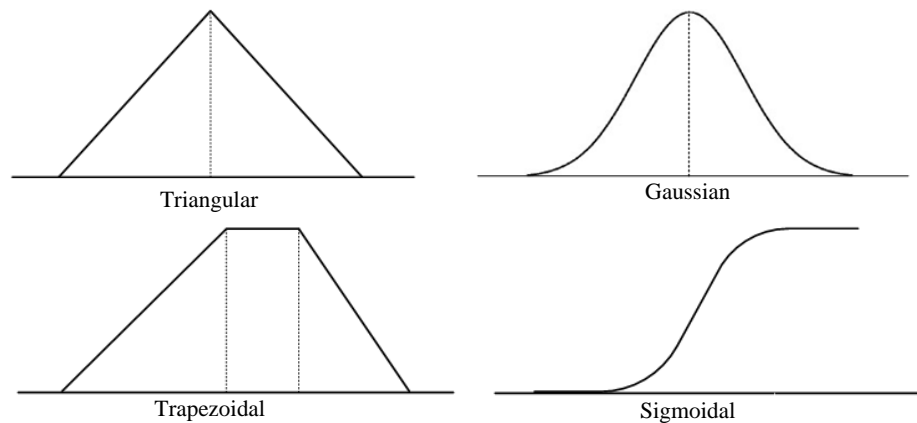


Figure 4: Different types of membership functions

There are many studies in which different types of fuzzy logic membership functions are used for both of the input and output variables. Some of them used only one type of membership functions as Hussein did who used the Gaussian membership function [37] and as Ramirez-Gonzalez did who used the triangular membership function [38]. Some of the researchers used more than one type of the membership functions as El-Metwally did in his paper when he used the sigmoid function on both sides and bell function in the middle for each input [39]. Other researchers compared between different types of the membership functions to select the best one for the input and output variables in designing the fuzzy logic based

PSS. In his paper, Sambariya compared the performance of FPSS when using trapezoidal (narrow "shoulder" and wide "shoulder"), triangular, bell-shaped (narrow "shoulder" and wide "shoulder"), Gaussian, two-sided Gaussian, sigmoid, polynomial- π and z membership functions for both the input and output variables. He found that the performance of power system stabilizer when using the Gaussian membership function is effective for all test conditions. Furthermore, he found that the FPSS performance when using the triangular membership function is almost same as when using the Gaussian membership function [40]. The triangular membership function is considered in this research for that last reason, and also as the triangular membership function is easy to implement and fast for computation as it is formed using only straight lines [41].

2.5 Measurement device of PSS inputs

Many researchers used the conventional measurement units to get the inputs of the PSS, either CPSS or FPSS. In the conventional measurement units, the supervisory control and data acquisition (SCADA) system usually is used. Conventional devices measures only the magnitudes of the voltage and current phasors [61].

Compared to the conventional measurement units, PMUs provide the synchronized and accurate measurements of the magnitude and angle of the current and voltage phasors in addition to the frequency and the rate of change of the frequency in a much higher speed and reporting rate. Using this characteristic, PMUs can be placed on different system buses and measurements can be taken and

compared with each other as they are taken simultaneously, so the overall picture of the interconnected power systems can be obtained in real time [14].

Table 1 provides a comparison between SCADA and PMUs systems.

Table 1: Comparison between SCADA and PMUs [61]

Attribute	SCADA	PMUs
Measurement	Analogue	Digital
Monitoring	Local	Wide- Area
Resolution	2-4 samples per cycle	About 60 samples per cycle
Observability	Steady State	Dynamic/Transient
Phasor Angle Measurement	No	Yes

In order to damp out the low frequency oscillations, the measurements of the PMUs, such as voltage, current, frequency and frequency deviation, can be used as input signals to the PSS.

2.6 Summary of the Literature Review

Table 2 includes the summary of the main points mentioned in the literature review.

Table 2: Literature review summary

Parameter	Pros	Cons
Conventional PSS	- Provides good performance around the operating point.	- It is tuned using linearized power system model for a specific operating point which when changed, the performance may degrade. - The designing of it requires mathematical modelling.
Fuzzy logic based PSS	- It performs more efficiently than the CPSS in varying environment for different operating points. - It doesn't require any complex mathematical modeling	- Due to the complexity and non-linearity of the power system, its designing require expert knowledge or offline simulation.
Input signals of the FPSS	- They can be the change of rotor speed ($\Delta\omega$), the rate of change of rotor speed ($\Delta\dot{\omega}$), the tie-line active power deviation (ΔP), the active power (P), reactive power (Q) and tie-line reactance (X_c). - $\Delta\omega$ is more appropriate input as the frequency of the system is independent of its configuration and operating procedures and the rotor speed will vary as the consumed power changes.	

Linguistic Control Variables	<ul style="list-style-type: none"> - As the total number of linguistic variables is increased, the precision of control will be better. - Seven linguistic variables may be enough which will compose up to 49 rules. 	<ul style="list-style-type: none"> - In addition to the increase in required memory, increasing the total number of the linguistic variables will also increase the computational time.
Membership Function	<ul style="list-style-type: none"> - The performance of FPSS with the Gaussian membership function is better than the other types. - FPSS performance with the triangular membership function is almost same as when using the Gaussian membership function. - The triangular membership function is easy to implement and fast for computation as it is formed using only straight lines 	<ul style="list-style-type: none"> - Implementation of the Gaussian membership function is more difficult than the triangular.
Measurement device of PSS inputs	<ul style="list-style-type: none"> - PMUs provide the synchronized and accurate measurements of the current and voltage phasors, frequency and the rate of change of the frequency in a much higher speed than the conventional units. 	<ul style="list-style-type: none"> - Conventional units provide measurements with slower rate which are not time synchronized.

2.7 Contributions of the Thesis

To the best of the author knowledge, there is no published research in which the researchers used both of Real-Time Digital Simulator (RTDS) and Phasor Measurement Unit (PMU) signals in designing and testing the FPSS. Hence, the contribution of the research reported in this thesis is to design an FPSS that will help in damping out the low frequency oscillations based on the global signals which are obtained from the PMUs. While the simulation was done using MATLAB/Simulink, the designed FPSS was implemented and tested based in real time using Real-Time Digital Simulator (RTDS).

Chapter 3: Power System Modeling and Methods of Analysis

To study a power system effectively, the best way is to apply the modal analysis to the linearized model of the system as well as the nonlinear simulation. In this thesis, the modal (eigenvalues) analysis has been performed to the linearized model of the 2-area power system to identify the inter-area oscillation mode with and without PSS for small disturbance such as gradual increase in the load. The nonlinear simulations has been done using MATLAB/Simulink model as well as RTDS system model with PMUs to show that the system recovers its transient stability after sever disturbance such as the three phase fault. This chapter sheds light on the mathematical models that describe the system dynamics.

3.1 Synchronous Generator Modeling

Synchronous machine is a type of a rotating electric machines in which the DC field winding is located on the rotor and AC armature winding is located on the stator. It can function as a generator (converts mechanical power to the electrical power) or as a motor (converts electrical power to mechanical power). It can be represented in different models (transfer functions) in order to study the dynamic and transient stability of the system. In the synchronous machines model, the dq-axes are used in the description of rotating electric machinery in order to simplify the mathematical analyses. Figure 5 shows the schematic diagram of three-phase synchronous machines with a representation of the damper winding on the rotor and stator along the direct axis (d) and the quadrature axis (q).

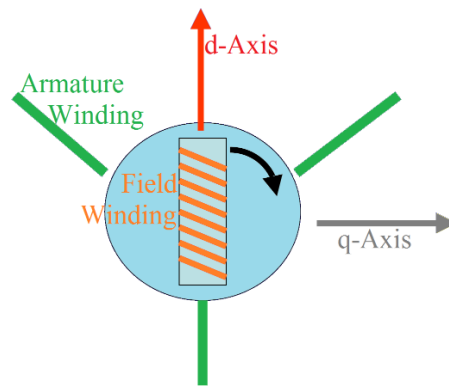


Figure 5: Schematic diagram of the synchronous machines

An 8th order model is considered as complete enough model of the synchronous generator with the required details. This model represented with six electrical nonlinear dynamic equations and two mechanical nonlinear dynamic equations. Since the salient pole synchronous generator has a lesser damper winding at q axis than the round pole synchronous generator 8th order model, so the full model order is 7 for it. However, it is very difficult to study a very detailed model of the synchronous generator as its behavior is so sophisticated and needs many state variables and sometimes the reduced order models are simpler versions of the same model. These reduced models can be obtained by neglecting the damper windings and transient flux linkages [42] and based on the required analysis, they can give very accurate results to study the dynamic stability in comparison with the full models which are more appropriate to study the transient stability [43].

Here is the brief description of different models of the round pole synchronous generator taking into consideration six state variables E_d'' , E_q' , ω , δ , E_d' , E_q'' , and subtransient reactance, X_q'' and X_d''

3.1.1 Four Winding Model (6th Order Model)

The 6th order model, which is also known as the four winding model, has two winding on the q-axis and another two windings on the d-axis. This model is actually the 8th order itself except that $\omega_r = \omega_s$ and the stator and network transients are neglected which leads to conservative results such action is desirable in stability studies [42].

The 6th order dynamic model of synchronous generator is described by the following differential equations [42].

$$T_{d0}' \frac{dE_q'}{dt} = -E_q' - (X_d - X_d') \left[I_d - \frac{X_d' - X_d''}{(X_d' - X_{ls})^2} (\psi_{1d} + (X_d' - X_{ls})I_d + E_q') \right] + E_{fd} \quad 3.1$$

$$T_{d0}'' \frac{d\psi_{1d}}{dt} = -\psi_{1d} + E_q' - (X_d' - X_{ls})I_d \quad 3.2$$

$$T_{q0}' \frac{dE_d'}{dt} = -E_d' - (X_q - X_q') \left[I_q - \frac{X_q' - X_q''}{(X_q' - X_{ls})^2} (\psi_{2q} + (X_q' - X_{ls})I_q + E_d') \right] \quad 3.3$$

$$T_{q0}'' \frac{d\psi_{2q}}{dt} = -\psi_{2q} + E_d' - (X_q' - X_{ls})I_q \quad 3.4$$

$$\frac{d\delta}{dt} = \omega - \omega_s \quad 3.5$$

$$\begin{aligned} \frac{2H}{\omega_s} \frac{d\omega}{dt} = & T_M - \frac{X_d'' - X_{ls}}{X_d' - X_{ls}} E_q' I_q - \frac{X_d' - X_d''}{X_d' - X_{ls}} \psi_{1d} I_q - \frac{X_q'' - X_{ls}}{X_q' - X_{ls}} E_d' I_d + \frac{X_q' - X_q''}{X_q' - X_{ls}} \psi_{2q} I_d - \\ & (X_q'' - X_d'') I_d I_q - T_{FW} \end{aligned} \quad 3.6$$

Equations 3.1-3.6 describe the four winding model. The first two equations represent the dynamics in the d axis while equations (3) & (4) represent the dynamics in the q axis. The swing equation is described in equation (5) and (6). T_{FW} introduces a damping torque proportional to the rotational speed [42].

3.1.2 Two-Axis Model (4th Order Model)

If the sub-transient time constants, T_{q0}'' and T_{d0}'' , set to be equal to zero as they are very small compared to the transient time constants, then the damper windings dynamics can be neglected and the two-axis model will be obtained that represented by the following equations [42].

$$T_{d0}' \frac{dE_q'}{dt} = -E_q' - (X_d - X_d') I_d + E_{fd} \quad 3.7$$

$$T_{q0}' \frac{dE_d'}{dt} = -E_d' - (X_q - X_q') I_q \quad 3.8$$

$$\frac{d\delta}{dt} = \omega - \omega_s \quad 3.9$$

$$\frac{2H}{\omega_s} \frac{d\omega}{dt} = T_M - E_q' I_q - E_d' I_d - (X_q' - X_d') I_d I_q - T_{FW} \quad 3.10$$

3.1.3 One-Axis Model (3rd Order Model)

In this model, the representation of the synchronous machine can be reduced further, so only the field winding will be remained. If the transient voltage in d-axis, E'_d , supposed to be constant, then the damping induced by eddy currents of the rotor body will be ignored and that will make $E'_d = 0$, $X'_q = X_d$ [44]. There is another justification for that which is inferred from the fact that the time constant T'_{q0} is small compared to T'_{d0} , so it can be equaled to zero, so the second equation in the 4th order model will be neglected. This model is selected to be used in this thesis.

The third order dynamic model of synchronous generator is described by the following equations [42].

$$T'_{d0} \frac{dE'_q}{dt} = -E'_q - (X_d - X'_d)I_d + E_{fd} \quad 3.11$$

$$\frac{d\delta}{dt} = \omega - \omega_s \quad 3.12$$

$$\frac{2H}{\omega_s} \frac{d\omega}{dt} = T_M - E'_q I_q - (X_q - X'_d)I_d I_q - T_{FW} \quad 3.13$$

3.1.4 Classical Model (2nd Order)

The classical model, which is also called constant flux linkage model, is the simplest model for the synchronous machine the field winding dynamics are neglected and describes only the dynamics of the rotor rotation. For that reason, the swing equation only will be required to describe the synchronous machine as it is

assumed that the voltage behind the transient reactance is constant. This model of synchronous generators is suitable for areas far from the disturbance in the very large power systems as it is not that much accurate [42].

$$\frac{d\delta}{dt} = \omega - \omega_s \quad 3.14$$

$$\frac{2H}{\omega_s} \frac{d\omega}{dt} = T_M - \frac{E'V_T}{X'_d} \sin(\delta - \theta_T) - T_{FW} \quad 3.15$$

Table 3 summarizes the states available in each of these 4 models.

Table 3: Summary of states in each model

State	2 nd Order	3 rd Order	4 th Order	6 th Order
$\frac{d\delta}{dt}$	✓	✓	✓	✓
$\frac{d\omega}{dt}$	✓	✓	✓	✓
$\frac{dE'_q}{dt}$		✓	✓	✓
$\frac{dE'_d}{dt}$			✓	✓
$\frac{dE''_q}{dt}$				✓
$\frac{dE''_d}{dt}$				✓

3.2 Turbine-Governor Model

The purpose of the turbine-governor is to sense the rotor speed and control the input fuel to keep the speed of the rotor constant to the required level. The turbine governor compares the control set point ΔP_C to the change of power consumed that is measured by the deviation in the frequency $\Delta\omega$ of the grid. If it is assumed that the deviation in frequency $\Delta\omega$ causes the change in power consumption proportionally, then the type of governor will be characterized as a proportional controller with a gain of $1/R$. The transfer function of the governor can be written as the following [15]:

$$\Delta P_v = \left(\frac{1}{1+s\tau_G} \right) \left(\Delta P_C - \frac{1}{R} \Delta\omega \right) \quad 3.16$$

where (τ_G) is the time constant of the governor.

The inputs of this model are the frequency deviation and the control set point, while the output is the valve position command ΔP_v that fed to a servomotor in order to adjust the valve through which the steam flows to the turbine [15].

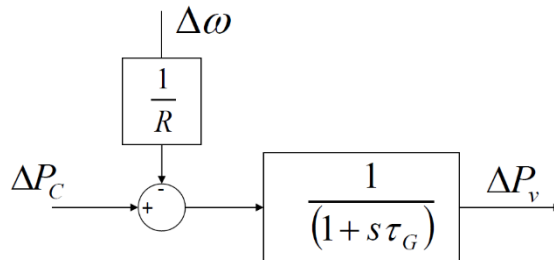


Figure 6: Governor model

3.3 Modeling of the Exciter

It's intended to use the AC type of excitation systems which consist of AC generator and either stationary or rotating rectifier to convert the alternate current to the direct current to excite the generator field. This type of excitation systems include 8 models which are [45]:

AC1A: Field-controlled alternator-rectifier excitation system and it consists of the alternator main separate exciter with diode rectifier (non-controlled).

AC2A: Same as AC1A except that it also includes the exciter field current limiting elements and exciter time constant compensation.

AC3A: Same as AC1A except that the exciter is self-excited and the voltage regulator power is derived from the exciter output voltage.

AC4A: Self-excited armature-supplied controlled-rectifier and there is a full thyristor bridge in the exciter output circuit (controlled). To control its output voltage to a constant value, the exciter alternator uses an independent voltage regulator. This modal is used in this study because it allows negative field current to allow de-excitation of the generator. It is illustrated in Figure 7.

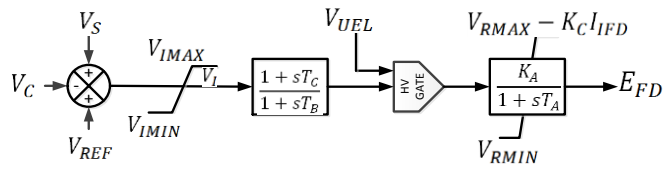


Figure 7: IEEE Type AC4A Excitation System Model

AC5A: It can be considered as the simplified model of the brushless excitation systems with separate excitation.

AC6A: This type represents the field-controlled alternator-rectifier excitation systems with system-supplied electronic voltage regulators.

AC7B: This model incorporates newer controls and PID controller with AC alternator and diode rectifier bridge.

AC8B: This model differs in the form of PID controller. Here, proportional, integral and differential gains are defined as separate constants [46].

3.4 PSS Modeling

The CPSS block diagram shown in Figure 8 which includes the following blocks [18]:

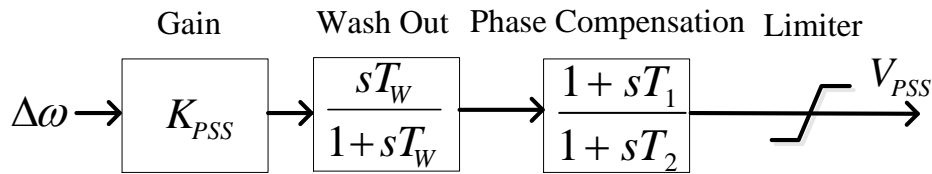


Figure 8: General block diagram of the conventional PSS

1. Gain block, which sets the limits for the amount of damping provided by the PSS.
2. A washout circuit block which can be considered as high pass filter that filters the low frequencies available in the input ($\Delta\omega$) signal and allows the PSS to respond only to speed oscillations rather than any DC offsets signal.
3. Phase compensation block, which supplies the proper lead-phase feature for compensating the input lag-phase between the exciter input and the generator electrical torque.
4. There is a limiter at the output to prevent V_{PSS} from driving the excitation into heavy saturation.

3.5 Transmission Line Models

The transmission line can be modeled in various models using series inductance, series resistance, shunt conductance and shunt capacitance. Those parameters are affected by the voltage level, type of conductor used, line length,

number of conductors, and the spacing of the conductors as they are mounted on the supporting structure [47]. However, the transmission line categorized by its length in the following models:

- Short line if its length is less than 80 km (50 mi).
- Medium line if its length is between 80 km (50 mi) and 240 km (150 mi).
- Long line if it is longer than 240 km (150 mi).

The medium line model has been used in this thesis and there are two configurations for this model, nominal π or nominal T configurations.

In the first configuration, nominal π , the shunt capacitance of the line is splitted into two equal parts, each part put on either ends of sending and receiving while the lumped series impedance is placed in the middle as in Figure 9 [48].

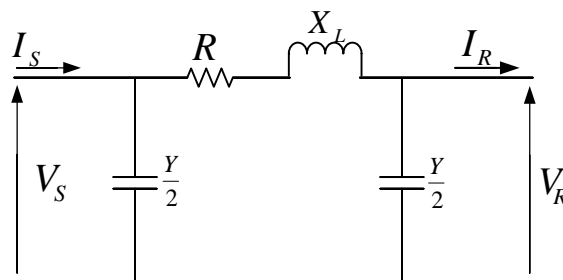


Figure 9: Medium transmission line representation, nominal π configuration

In the nominal T representation, the shunt capacitance of the line is placed in the middle while the series impedance is splitted into two equal parts and placed on either sides of the shunt capacitance as in Figure 10 [48].

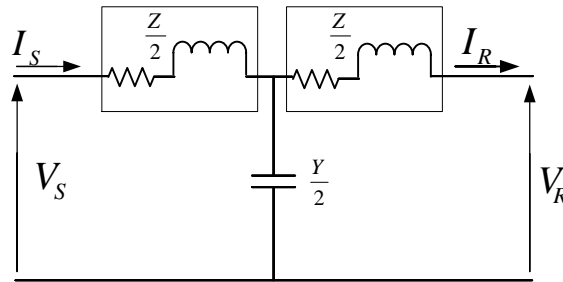


Figure 10: Medium transmission line representation, nominal T configuration

3.6 Load Model

For load modelling, static load model selected as it is easy to see the effect of the load on the system stability. The static load model can be represented by the following two exponential equations of active power, p , and reactive power, Q :

$$P = P_0 \left(\frac{V}{V_0} \right)^\alpha \quad 3.17$$

$$Q = Q_0 \left(\frac{V}{V_0} \right)^\beta \quad 3.18$$

where P_0 and Q_0 represent the initial value of the power consumed by the load at voltage V_0 .

$\alpha=\beta=0$ for the constant power load. Both of them are 1 for the constant current load while they are 2 for the constant impedance load [49].

3.7 Linearization of the Power System Model

The stated models in this chapter are non-linear which can be linearized around the operating point where the system performance is very good. Hence linear system analysis and control techniques such as s domain and pole placement can be used.

3.7.1 Generator linearization

The third order model of synchronous generator which is selected in this thesis can be linearized starting from the dynamical model as the following:

$$T'_{do} \frac{dE'_q}{dt} = -E'_q - (X_d - X'_d)I_d + E_{fd} \quad 3.19$$

$$\frac{d\delta}{dt} = \omega - \omega_s \quad 3.20$$

$$\frac{2H}{\omega_s} \frac{d\omega}{dt} = T_M - T_e - T_{FW} \quad 3.21$$

$$\text{where } T_e = E'_q I_q - (X_q - X'_d) I_d I_q \quad 3.22$$

Stator Equations:

$$V_t \sin(\delta - \theta) - X_q I_q = 0 \quad 3.23$$

$$V_t \cos(\delta - \theta) + X'_d I_d - E'_q = 0 \quad 3.24$$

From equation (3.22), (3.23) and (3.24)

$$I_q = \frac{V_t \sin(\delta - \theta)}{X_q} \quad 3.25$$

$$I_d = \frac{E'_q - V_t \cos(\delta - \theta)}{X'_d} \quad 3.26$$

$$\Delta I_q = \frac{V_t \cos(\delta - \theta)}{x_q} \Delta \delta \quad 3.27$$

$$\Delta I_d = \frac{\Delta E'_q}{X'_d} + \frac{V_t \sin(\delta - \theta)}{X'_d} \Delta \delta \quad 3.28$$

From equation (3.25), (3.26), (3.27) and (3.28)

$$\begin{aligned} I_d I_q = & \left[\frac{E'_q - V_t \cos(\delta - \theta)}{X'_d} \right] \left[\frac{V_t \cos(\delta - \theta)}{X_q} \Delta \delta \right] \\ & + \left[\frac{\Delta E'_q}{X'_d} + \frac{V_t \sin(\delta - \theta)}{X'_d} \Delta \delta \right] \left[\frac{V_0 \sin(\delta_0 - \theta_0)}{X_{q0}} \right] \end{aligned} \quad 3.29$$

Finally the Linearized equations

$$\Delta \dot{E}'_q = -\frac{1}{T'_{d0}} \Delta E'_q - \frac{1}{T'_{d0}} (X_d - X'_d) \Delta I_d + \frac{1}{T'_{d0}} \Delta E_{fd} \quad 3.30$$

$$\Delta \dot{\delta} = \omega_B \Delta \omega \quad 3.31$$

$$\Delta \dot{\omega} = \frac{1}{2H} T_M - \frac{1}{2H} \Delta T_e \quad 3.32$$

3.7.2 Exciter Model Linearization

For the simplified model of IEEE AC4A excitation that is shown in Figure 11 [50], the linearized equation is:

$$\Delta E'_{fd} = \frac{1}{T_A} \left(-\Delta E_{fd} + K_A (\Delta V_{ref} - \Delta V_t) \right) \quad 3.33$$

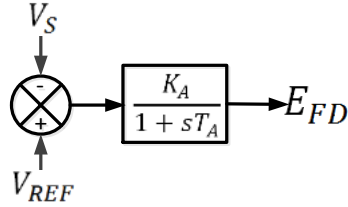


Figure 11: IEEE Type AC4A Excitation System Model

3.7.3 Linearization of PSS

For the model of CPSS in Figure 8:

$$\Delta V_{s1} = (K_{pss} \frac{sT_w}{1 + sT_w}) \Delta \omega \quad 3.34$$

$$\Delta V_{s1} + \Delta \dot{V}_{s1} T_w = K_{pss} T_w \Delta \dot{\omega}$$

$$\Delta \dot{V}_{s1} = K_{pss} \Delta \dot{\omega} - \frac{1}{T_w} \Delta V_{s1} \quad 3.35$$

$$\frac{\Delta V_{s2}}{\Delta V_{s1}} = \frac{1 + sT_1}{1 + sT_2} \quad 3.36$$

$$\Delta V_{s2} + T_2 \Delta \dot{V}_{s2} = \Delta V_{s1} + T_1 \Delta \dot{V}_{s1} \quad 3.37$$

$$\Delta \dot{V}_{s2} = \frac{-1}{T_2} \Delta V_{s2} + \frac{1}{T_2} \Delta V_{s1} + \frac{T_1}{T_2} \Delta \dot{V}_{s1} \quad 3.38$$

$$= \frac{-1}{T_2} \Delta V_{s2} + \frac{1}{T_2} \Delta V_{s1} + \frac{T_1}{T_2} \left(K_{pss} \Delta \dot{\omega} - \frac{1}{T_w} \Delta V_{s1} \right)$$

$$= \frac{-1}{T_2} \Delta V_{s2} + \frac{1}{T_2} \Delta V_{s1} + \frac{T_1 K_{pss}}{T_2} \Delta \dot{\omega} - \frac{T_1}{T_2 T_w} \Delta V_{s1}$$

$$= \frac{-1}{T_2} \Delta V_{s2} + \left(\frac{1}{T_2} - \frac{T_1}{T_2 T_w} \right) \Delta V_{s1} + \frac{T_1 K_{pss}}{T_2} \Delta \dot{\omega}$$

3.8 Modal Analysis

Before applying the modal analysis, the linearized dynamic system model should be represented in the state space form as in equation 3.22:

$$\Delta \dot{x} = A \Delta x + B \Delta u \quad 3.39$$

Δx is the state vector which includes the linearized state-variables and Δu is the input vector of all generators.

In the modal analysis, the system eigenvalues λ_i of an oscillatory mode i can be represented as in equation 3.40:

$$\lambda_i = \alpha_i \pm j\omega_i \quad 3.40$$

where α is the damping coefficient and ω is the frequency of the oscillation, rad/sec which can be divided by 2π to obtain the frequency in Hz.

The rate on which the amplitude of the oscillation decays can be obtained from the damping ratio ζ_i where:

$$\zeta_i = \frac{-\alpha_i}{\sqrt{\alpha_i^2 \pm \omega_i^2}} \quad 3.41$$

3.8.1 Assessment of the Stability Using Modal Analysis

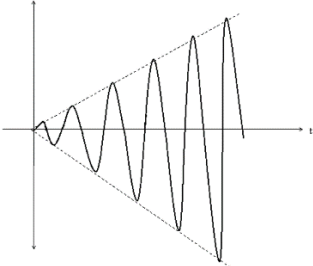
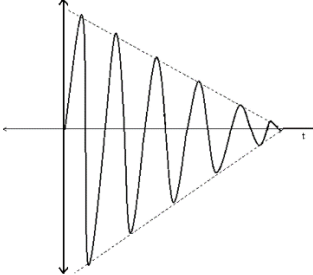
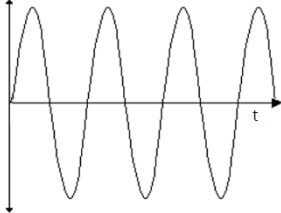
Eigenvalue can be used to check whether the system is stable or unstable. The system is said to be stable if its all eigenvalues are negative real numbers or complex numbers with negative real part, α . In general, there are three possibilities for eigenvalues of the system:

- If any eigenvalue has a negative real part, then the system is stable as the negative real part of eigenvalue indicates a positive damping that leads the oscillations to be decaying.

- If any eigenvalue has a positive real part, then the system is unstable as the positive real part indicates negative damping that leads the oscillations to be increasing.
- If any eigenvalue has an imaginary part, then the system oscillates with constant amplitude around the steady state.

Table 4 describes the effects of eigenvalue on the system and it can indicate the stability of power system.

Table 4: Eigenvalue and system stability

Eigenvalue	Effect of eigenvalue on the system	System response
Complex with + real number	Oscillates with increasing amplitude	 <p>The graph shows a sinusoidal wave on a coordinate system with a vertical axis and a horizontal axis labeled 't'. The amplitude of the wave increases as time progresses, forming an expanding envelope that starts from the origin and grows outwards.</p>
Complex with - real number	Oscillates with decreasing amplitude	 <p>The graph shows a sinusoidal wave on a coordinate system with a vertical axis and a horizontal axis labeled 't'. The amplitude of the wave decreases as time progresses, forming a contracting envelope that starts from a large initial amplitude and tapers towards the horizontal axis.</p>
Imaginary	Oscillates with constant amplitude	 <p>The graph shows a sinusoidal wave on a coordinate system with a vertical axis and a horizontal axis labeled 't'. The amplitude of the wave remains constant over time, forming a steady, repeating oscillation.</p>

Chapter 4: FPSS Design Based on PMU Signals

The design of any fuzzy based controller has the following four interfaces:

1. Fuzzification: The real numerical values of the control signals should be transformed into suitable linguistic values using different types of membership functions.
2. Rule-base: In this interface, the rule-base for each control signal will be defined in terms of set of linguistic control rules.
3. Decision-making logic: In this part, the human decision-making procedure will be simulated based on fuzzy concepts.
4. De-Fuzzification: In this part, the output will be returned back from the linguistic value to the non-fuzzy value that best stands for the possibility distribution of a fuzzy control action inferred.

This chapter is dedicated to illustrate the design steps of the FPSS.

4.1 State and Control Variables

Based on the literature review, the fuzzy based PSS that will be designed has two inputs which are the frequency deviation (Δf) and its differentiation ($\Delta \dot{f}$) and a single output that represents the stabilizing signal (v_s). The block diagram in Figure 12 illustrate the stages of the FPSS.

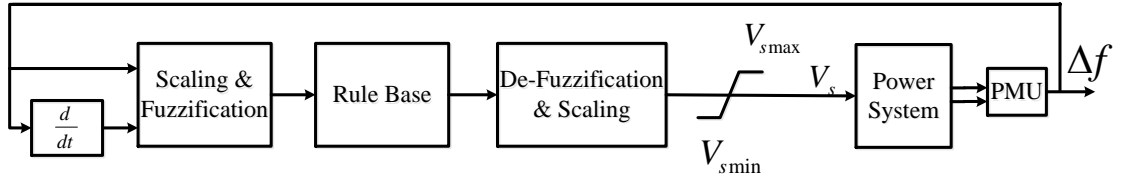


Figure 12: FPSS block diagram

Δf can be obtained from the measurements of the PMUs and this represents the signal of the error (e).

$\Delta \dot{f}$ can be derived from Δf at two consecutive sampling instants as below.

$$\Delta \dot{f}(kT) = \frac{\Delta f(kT) - \Delta f((k-1)T)}{T} \quad 5.1$$

where T_s is the sampling time and k is the sampling count [51]. Here, T_s assumed to be 1, so, above equation reduced to:

$$\Delta \dot{f}(kT) = \Delta f(k) - \Delta f(k-1) \quad 5.2$$

$\Delta \dot{f}$ represents the change of the error (ce).

The output of the FPSS represents the control variable (V_s) which will be applied to the excitation system in order to damp out the power low frequency oscillations.

4.2 Fuzzification

The state variables (Δf and $\Delta \dot{f}$) are then fed to the block of (Scaling and Fuzzification) in which the input control variables are read and scaled and then their original numerical measured values are transformed to the corresponding fuzzy linguistic variables with the suitable membership values using the rule-base in which the Mamdani inference method is selected to be used as it is simple and easy to implement.

4.3 Rule-Base Design

After conducting literature review, the set of rules that define the relation between the inputs and the output was made using seven linguistic variables which are BN (Big Negative), MN (Medium Negative), SN (Small Negative), (Zero), SP (Small Positive), MP (Medium Positive) and BP (Big Positive).

Since the power systems are so non-linear and complicated, fuzzy rule-base can be obtained either from the deep understanding of the behavior of the system (by an expert) or by a try and error method, using a simulation tool, till achieving the optimum results [56] [57] [58]. The latest method used in this thesis using simulation tool equipped with the RTDS and MATLAB/Simulink in such manner that makes the output of the FPSS to be able to reduce the negative damping that is injected by the AVR, so the low frequency oscillations will be reduced. For example, Figure 13 depicts the response of the power transmitted between the two areas in the two-area power system presented in Figure 19 under three-phase to ground fault at Bus 8 using the rule-base given in Table 5.

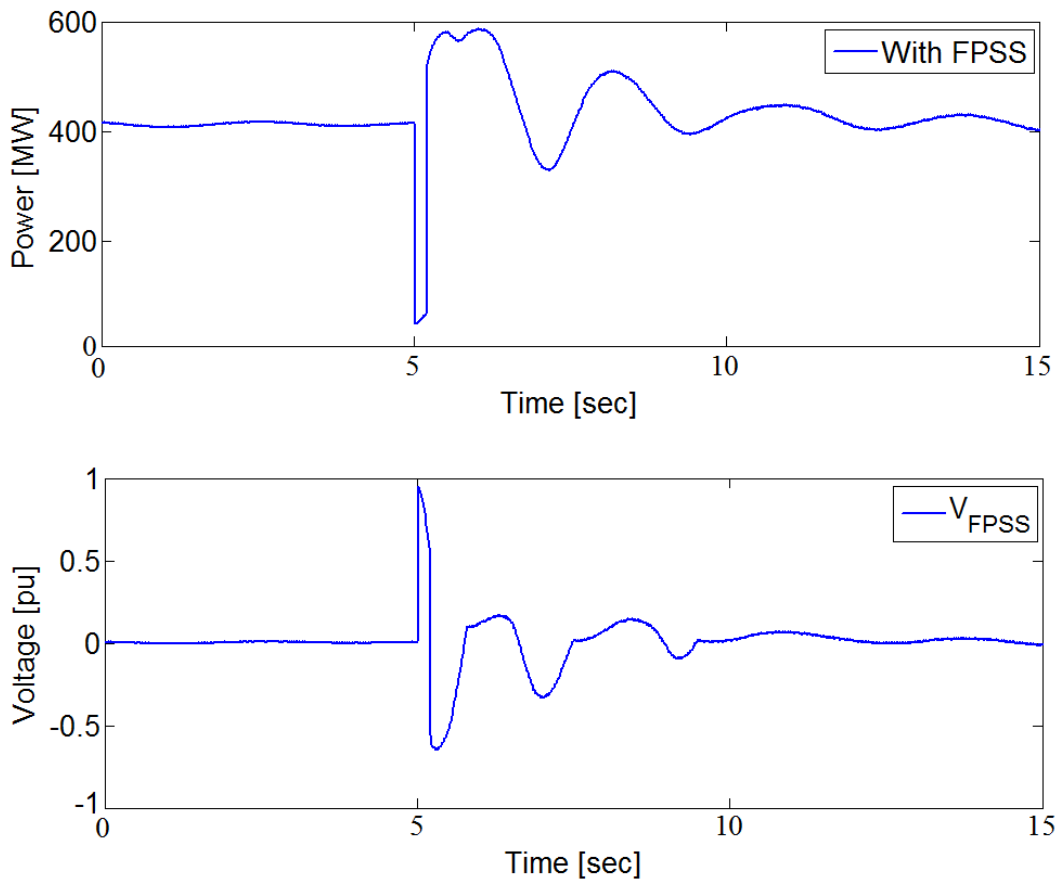


Figure 13: Response of the power transmitted between the areas in the two-area power system and the output signal of the FPSS (V_s)

Table 5: Raw rule-base for FPSS

		Frequency Deviation (Δf)							
		BN	MN	SN	Z	SP	MP	BP	
Rate of Change of Frequency Deviation ($\Delta \dot{f}$)	BN	BN	BN	MN	SN	SN	SN	SN	Z
	MN	BN	MN	SN	SN	SN	Z	SP	
	SN	MN	SN	SN	Z	Z	Z	SP	
	Z	SN	SN	Z	Z	Z	SP	SP	
	SP	SN	Z	Z	Z	SP	SP	MP	
	MP	SN	Z	SP	SP	SP	MP	LP	
	BP	Z	SP	SP	SP	MP	LP	LP	

Similarly, many other rule-bases have been tested using RTDS and Simulink till getting a reasonable good response with the rule-base presented in Table 6. This rule-bas has been used in this thesis to define the relation between the inputs and the output. The structure of the rules may look like:

Rule 1: If Δf is BN, AND $\Delta \dot{f}$ is BN, then V_S is also BN.

Rule 2: If Δf is BP, AND $\Delta \dot{f}$ is Z, then V_S is also MP.

Table 6: Final rule-base for FPSS

		Frequency Deviation (Δf)						
		BN	MN	SN	Z	SP	MP	BP
Rate of Change of Frequency Deviation ($\Delta \dot{f}$)	BN	BN	BN	BN	MN	MN	SN	Z
	MN	BN	MN	MN	MN	SN	Z	SP
	SN	BN	MN	SN	SN	Z	SP	MP
	Z	MN	MN	SN	Z	SP	MP	MP
	SP	MN	SN	Z	SP	SP	MP	BP
	MP	SN	Z	SP	MP	MP	MP	BP
	BP	Z	SP	MP	MP	BP	BP	BP

4.4 Inputs and output Membership Functions

Input variables are classified by inputs membership function that consists of trapezoidal and triangular shapes. The range has been defined as symmetrical between -1 to 1 (normalized) for both of Δf and $\Delta \dot{f}$ by multiplying the variables by appropriate scaling factors (gains). Each membership function overlaps with adjacent membership functions by 50%, as in Figure 14. The trapezoidal membership function is used in the upper and the lower boundary to make sure that any numerical inputs above or below the range of (-1 to 1) are taken to be BN and

BP respectively. Hence, the range of each of the memberships in the middle (MN, SN, Z, SP, and MP) is $2/3=0.66$.

The error (Δf) normalization scaling factor (or gain) is obtained through the RTDS/Simulink simulation, in such manner that helps in keeping the error within 1 and -1, so it will not enter the saturation region. On the other hand, the rate of change of error ($\Delta \dot{f}$) normalization scaling factor is obtained by calculating the slope of the highest obtained error.

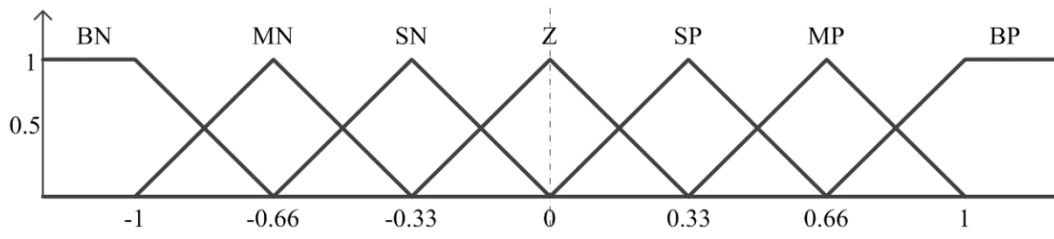


Figure 14: Membership function of the inputs/output normalized from -1 to 1

The triangles membership function were obtained using equation 5.3 [52].

Table 7 shows equations in details.

$$f(x, a, b, c) = \left\{ \begin{array}{ll} 0, & x \leq a \\ \frac{x-a}{b-a}, & a \leq x \leq b \\ \frac{c-x}{c-b}, & b \leq x \leq c \\ 0, & c \leq x \end{array} \right\} \quad 5.3$$

Table 7: Falling and Rising Sides of the membership function

Falling sides		Rising Sides	
BN	$-3x-2$	MN	$3x+3$
MN	$-3x-1$	SN	$3x+2$
SN	$-3x$	Z	$3x+1$
Z	$-3x+1$	SP	$3x$
SP	$-3x+2$	MP	$3x-1$
MP	$-3x+3$	BP	$3x-2$

In order to reduce the computational time/overhead, the whole membership equations in Table 7 have been merged or combined based on common areas/overlap.

4.5 De-Fuzzification

The output of the FPSS is de-fuzzified to the non-fuzzy numerical value based on the output membership function using the Weighted Average method, as the used membership function is symmetrical. In this method, the de-fuzzified results obtained by weighting each function in the output by its respective maximum membership value as in equation 5.4 [53].

$$z^* = \frac{\sum \mu_C(\bar{z}) \cdot \bar{z}}{\sum \mu_C(\bar{z})} \quad 5.4$$

The output should be scaled by a factor in order to de-normalize the output signal and to make sure that the range of outputs of the plant will not saturate.

4.6 Output Signal

The single output of the FPSS that represents the stabilizing signal (v_s) will be fed to the excitation system.

4.7 FPSS in MATLAB/Simulink

The model of the designed FPSS that has been built in MATLAB/Simulink is shown in Figure 15.

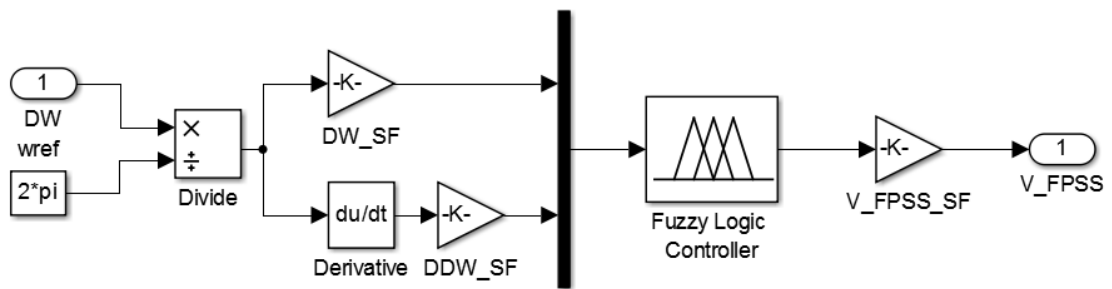


Figure 15: FPSS block diagram in MATLAB/Simulink

The block of Fuzzy Logic Controller has been built using Membership Function Editor as shown in Figure 16.

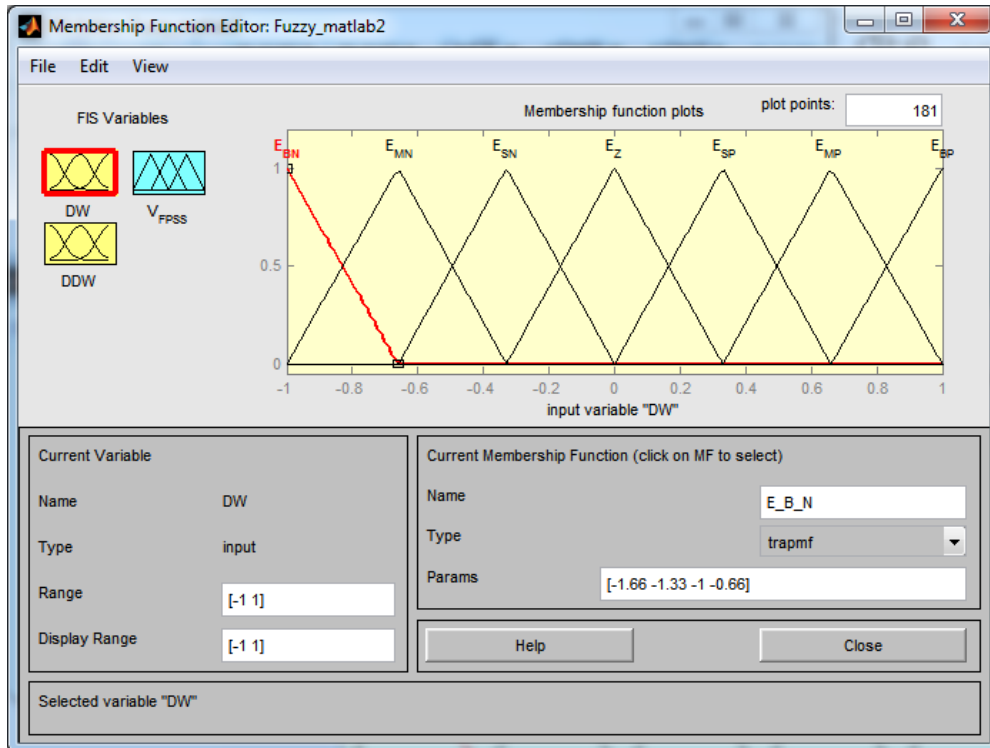


Figure 16: Inputs and output membership function

The rules that relate the inputs to the outputs which presented in Table 6 have been entered using the Rule Editor as in Figure 17.

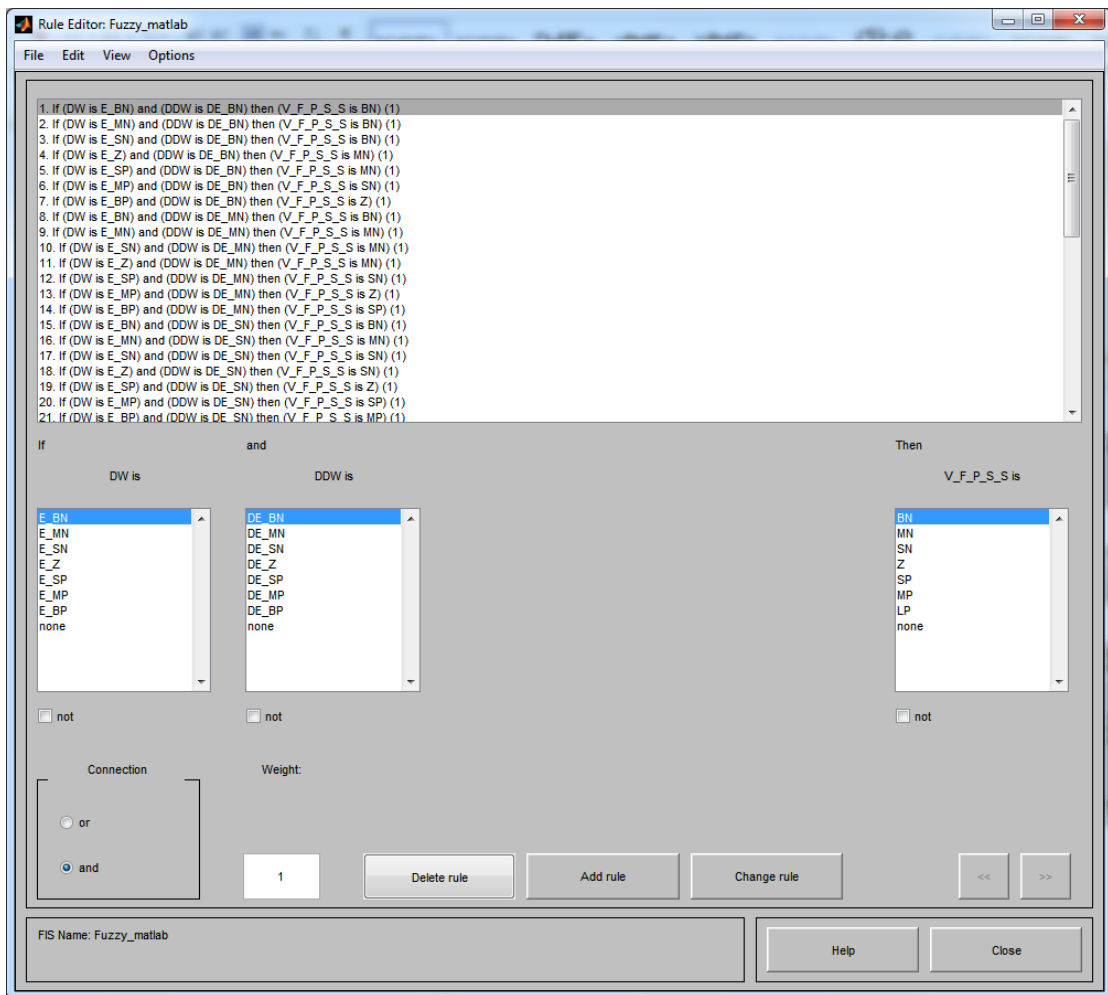


Figure 17: Rules that relate inputs to the outputs

4.8 Practical Implementation of the FPSS

The Fuzzy Based Power System Stabilizer has been developed/implemented by an ARM cortex M-4 Microcontroller shown in Figure 18 with the stated set of rules according to the steps that mentioned. The code that is used in programming is attached in Appendix E.

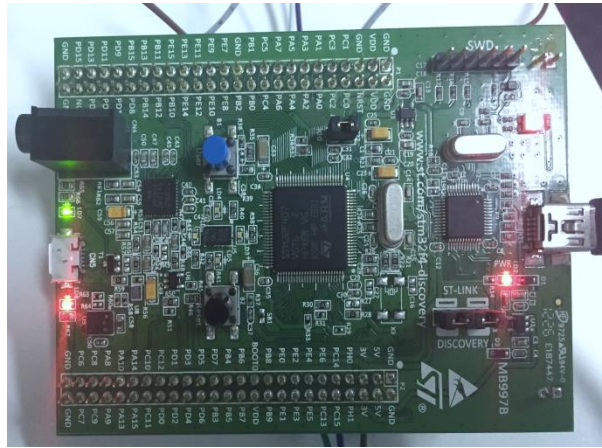


Figure 18: ARM μ -controller

Chapter 5: MATLAB/Simulink Simulation

Electric power system is non-linear system as its behavior description is done using non-linear differential-algebraic equations which contain many nonlinearities such as multiplication, trigonometric functions and limits on controller action. For that reason, the linearized methods (such as eigenvalues) are not enough to study the power system as those methods ignore the non-linearities of it. Hence, there is need to test the dynamic behavior of the power system through the time-domain simulations by applying different disturbances such as fault and the loss of a generating unit.

In this chapter, the designed FPSS has been tested and its performance in damping the low frequency oscillations compared with the conventional PSS, which is tuned by Kundur, using MATLAB/Simulink model. The time domain simulation of the tie-line power has been compared with what was obtained in [60].

5.1 Two-Area Power System

To test the robustness of the designed FPSS, the two-area power system model proposed by Kundur in [16] which is shown in Figure 19 has been used.

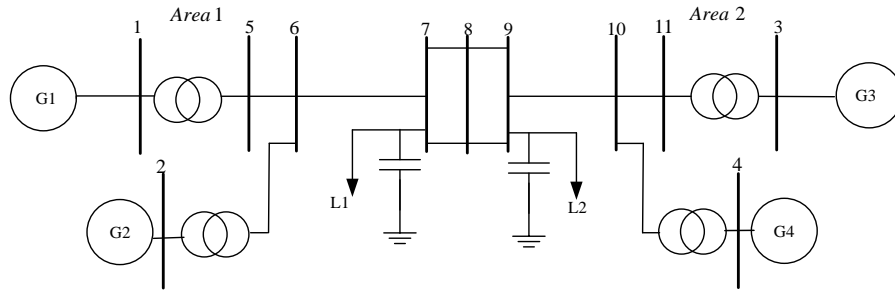


Figure 19: One-line diagram of the 4-machine 2-area power test system with PMU in each area

It consists of two groups of round rotor type generators representing two areas which are identical. Area 1 includes generators G1 and G2, while area 2 includes generators G3 and G4 and both areas are connected by a weak tie line (two 230 kV lines) which length is 220 km.

Each generator rate is 900MVA with 20KV and the following the parameters in per units:

$$T'_{d0} = 8.0 \text{ sec}, X_d = 1.81 \text{ pu}, X_q = 1.76 \text{ pu}, X'_d = 0.3 \text{ pu}, H = 6.5 \text{ sec}$$

(area 1 generators) and $H=6.175$ (area 2 generators), $\omega_s = 377 \text{ rad/sec}$

The amount of active power that is transferred from Area 1 to Area 2 is 413 MW. Each generator load is 700 MW and Area 1 load is about 967 MW while Area 2 load is 1767 MW [54].

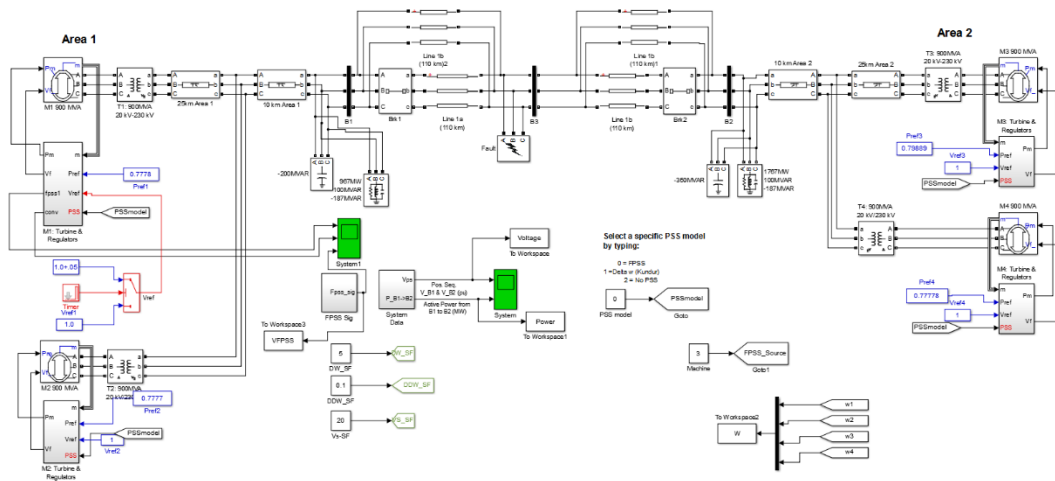


Figure 20: Simulink model of the two-area power system

5.2.1 System Behavior without PSS

The first scenario was to test the system without any PSS. A three phase to ground fault has been applied at the middle of the tie-line between the two areas (at bus 8) at time $t = 5$ sec and cleared with a fault clearing time of 0.200 sec. The time domain simulations were obtained for the active power transferred from area 1 to area 2, the voltage at bus 8 and the rotor speed of each machine.

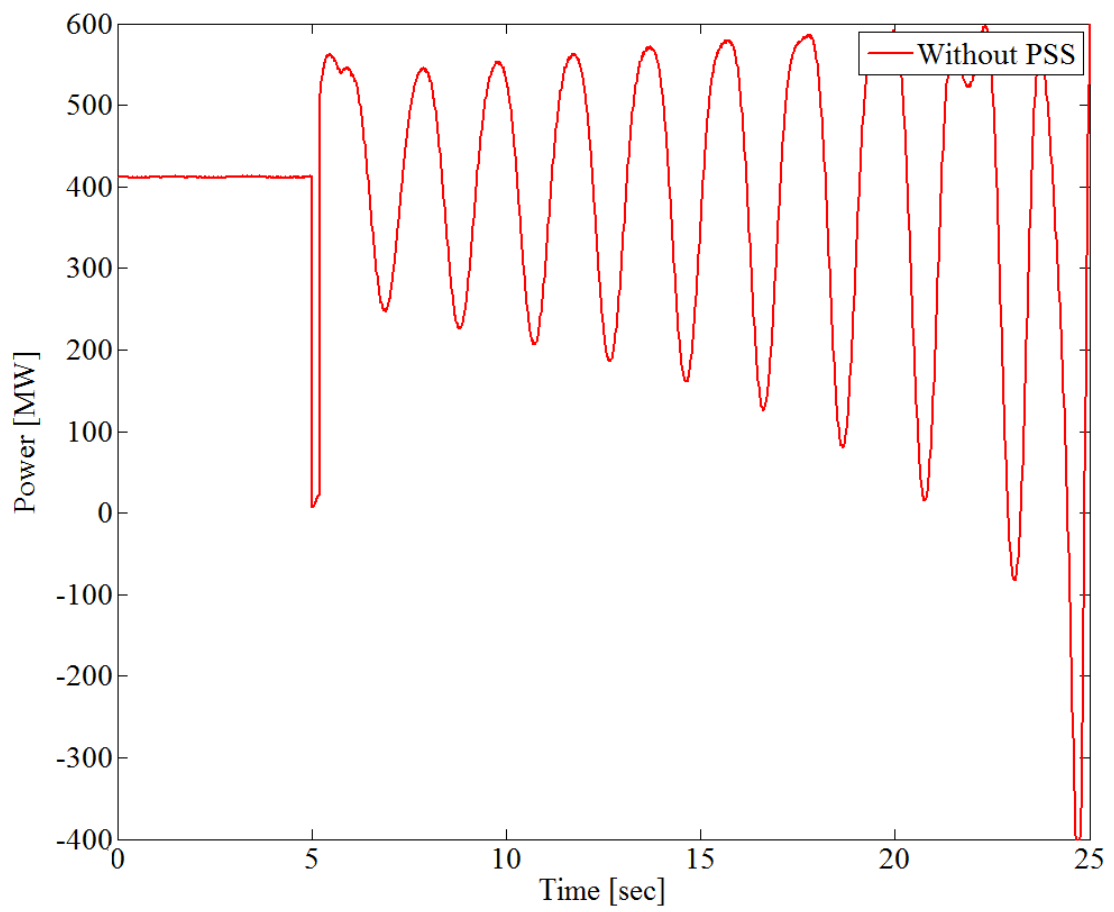


Figure 21: Response of the power exported from area 1 to area 2 without PSS

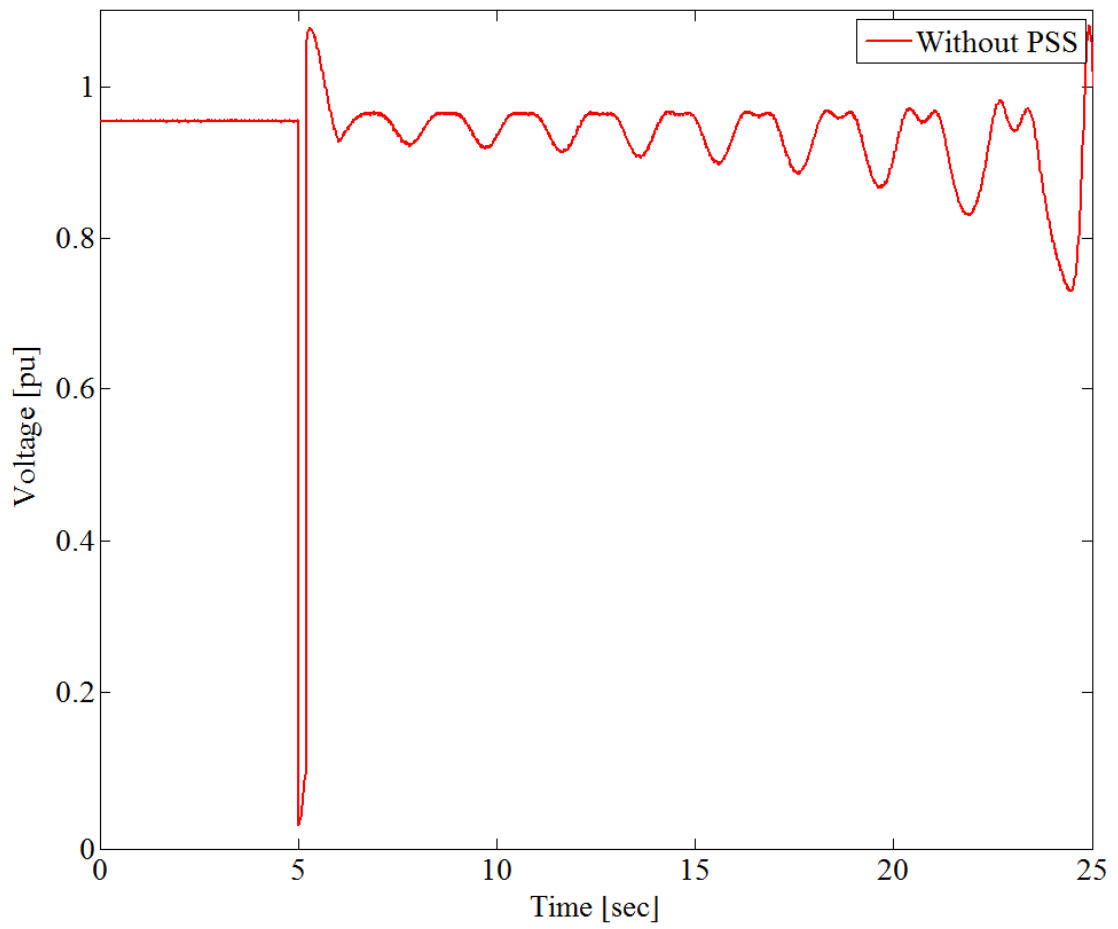


Figure 22: Response of voltage at bus 8 without PSS

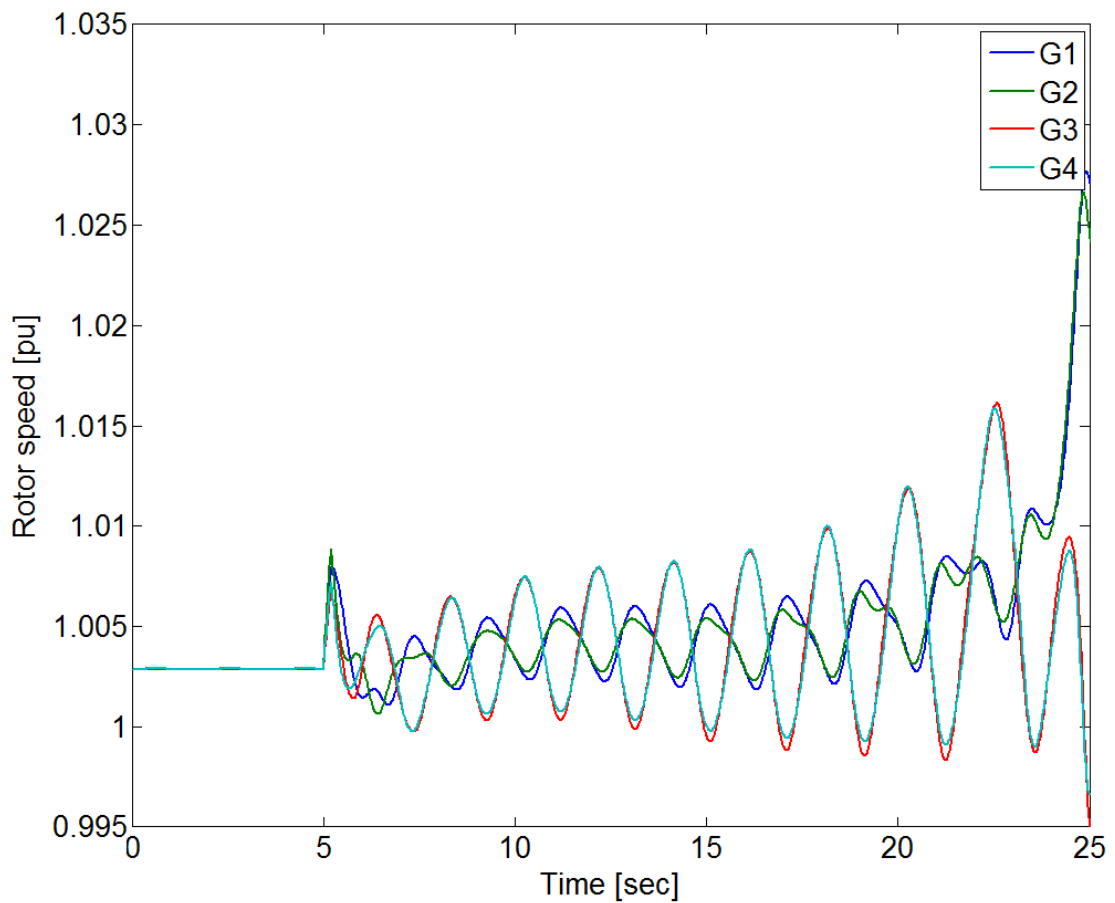


Figure 23: Response of the rotor speed for the four generators without PSS

It is obvious from Figures 21-23 that the system is unstable after the fault in the absence of the PSS. Also, it can be noticed from Figure 23, that the generators at area 2 swing out of phase of the generators in area 1.

5.3.1 System Behavior with PSS

Again, using MATLAB/Simulink model, a three phase to ground fault has been applied at the middle of the tie-line between the two areas (at bus 8) at time t

= 5 sec and cleared after 0.200 sec in the presence of PSS at Generator 1 only. The time domain simulations are presented in Figures 24-28.

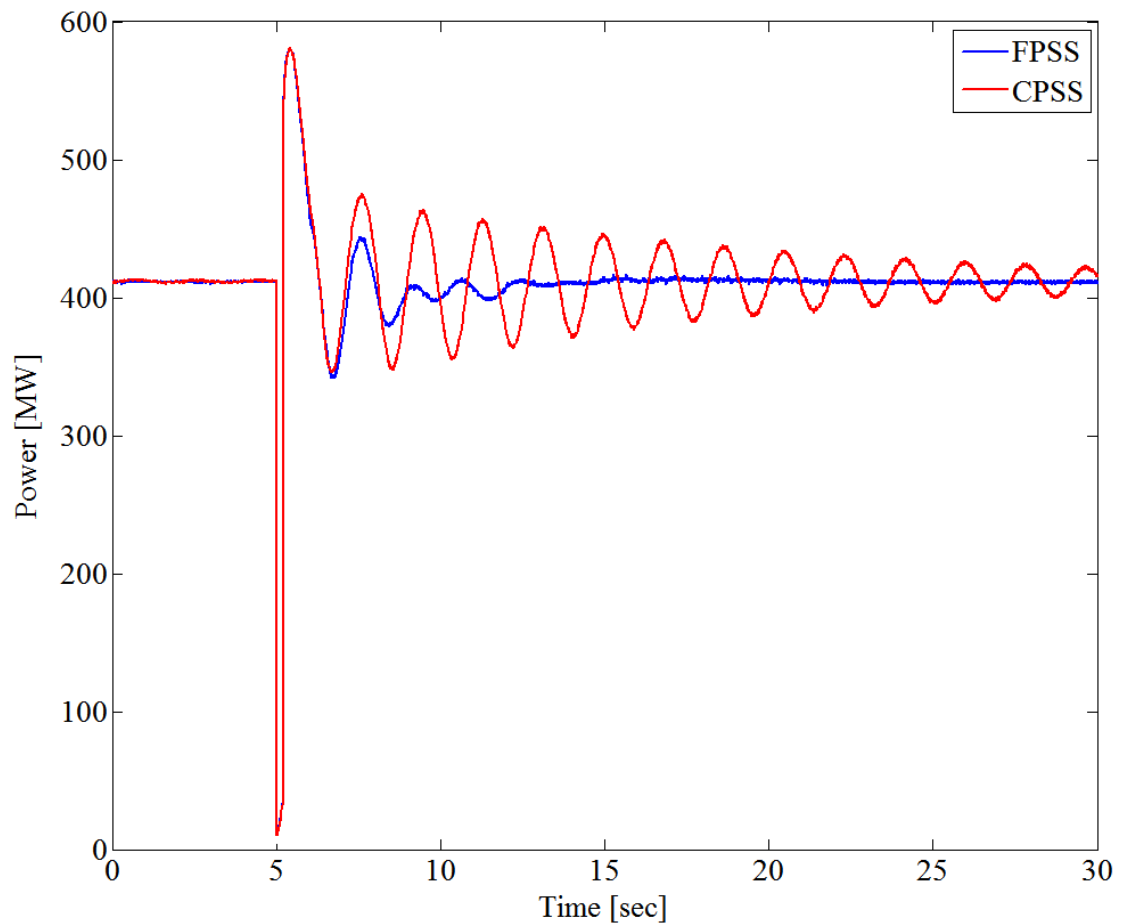


Figure 24: Response of the power exported from area 1 to area 2

From Figure 24, it can be noticed that the fuzzy PSS shows better damping for the low frequency oscillations than the CPSS. Although the maximum overshoot is almost the same, FPSS damped out the oscillations in about 8 sec after the fault

while the CPSS needed more than 30 sec to damp out these oscillations even though the inputs for both of them are same.

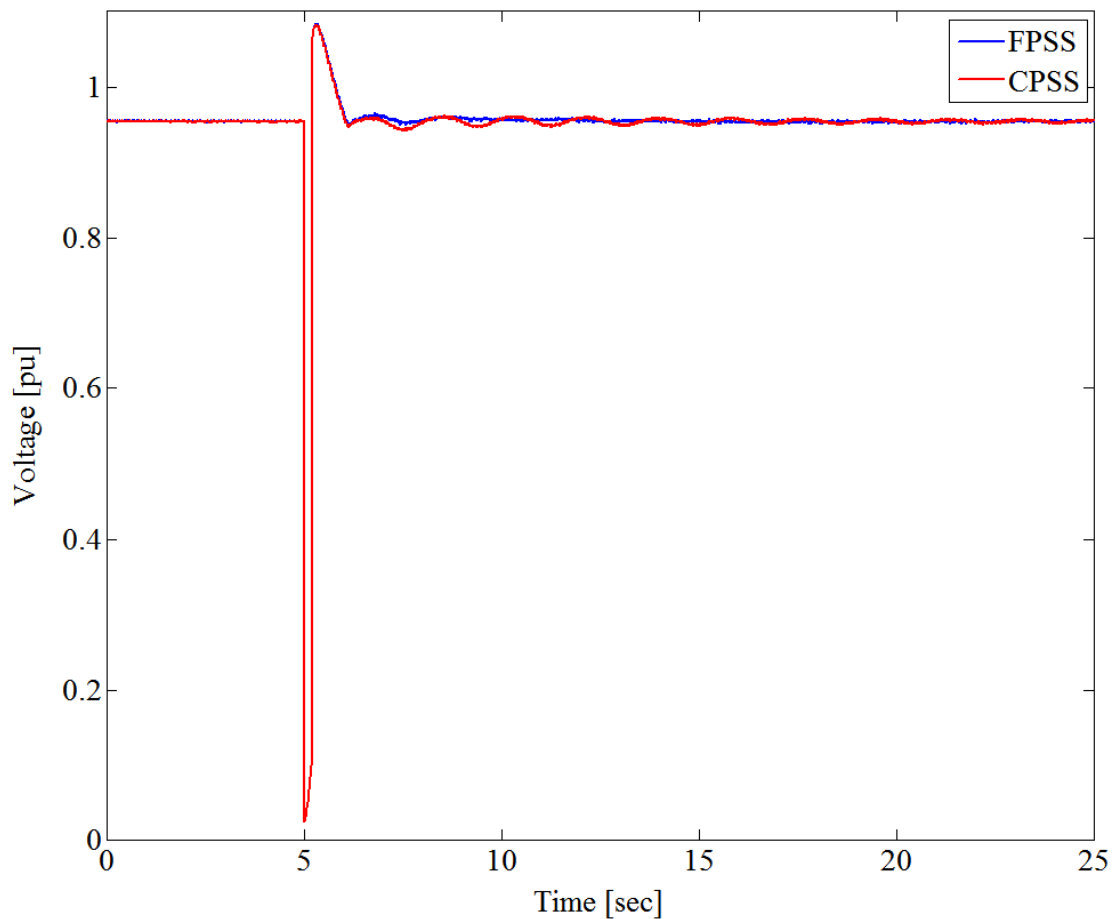


Figure 25: Response of voltage at bus 8 for a fault of 0.200 sec

From Figure 25, it can be noticed that the settling time for the voltage at the Bus 8 with the designed FPSS is much less than with the CPSS.

The response of the rotor speed of the generators are shown in Figures 26-28.

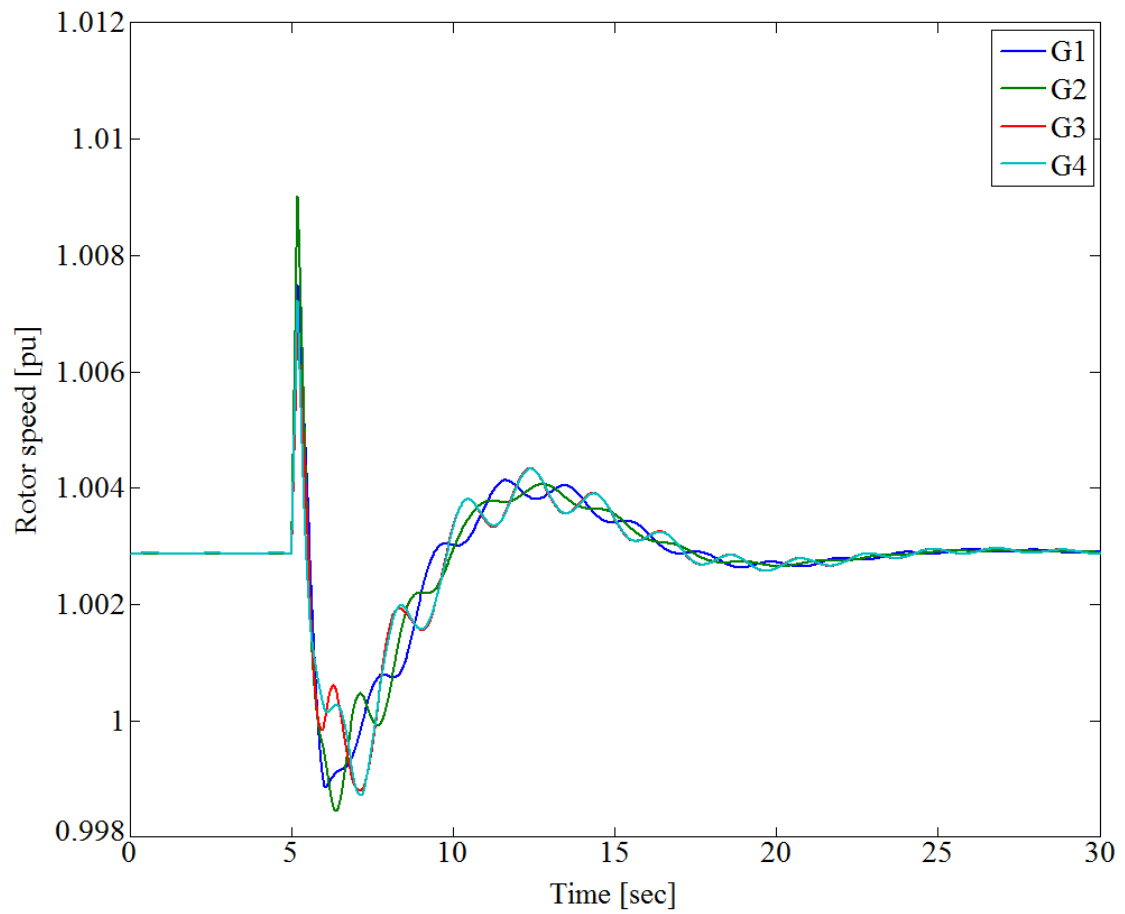


Figure 26: Response of the rotor speed of the four generators in presence of the designed FPSS

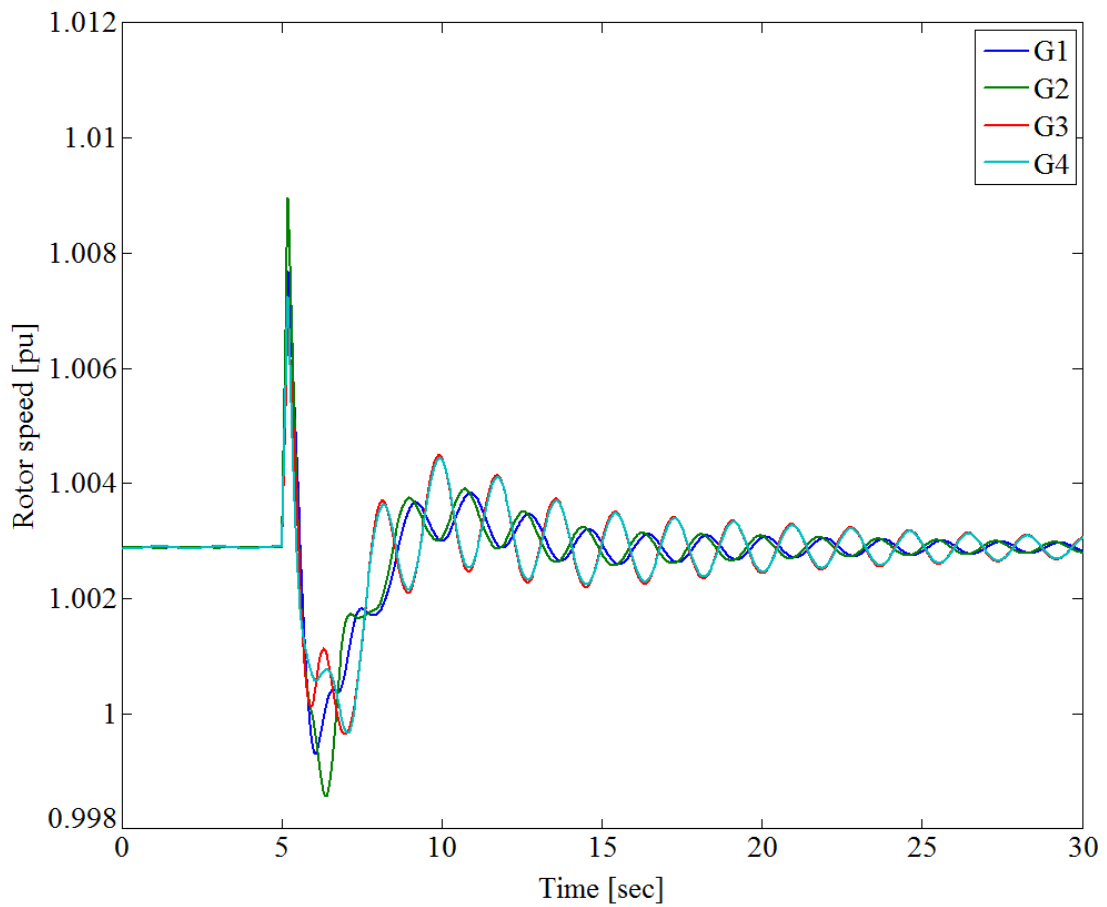


Figure 27: Response of the rotor speed of the four generators in presence of the CPSS

From Figures 26 and 27, it can be concluded that the rotors of the generators attained their nominal speed more quickly with the presence of the FPSS than with the presence of the CPSS. For comparison, the time simulation of the rotor speed of Machine 1 in area 1 and Machine 3 in area 2 are presented together in Figure 28.

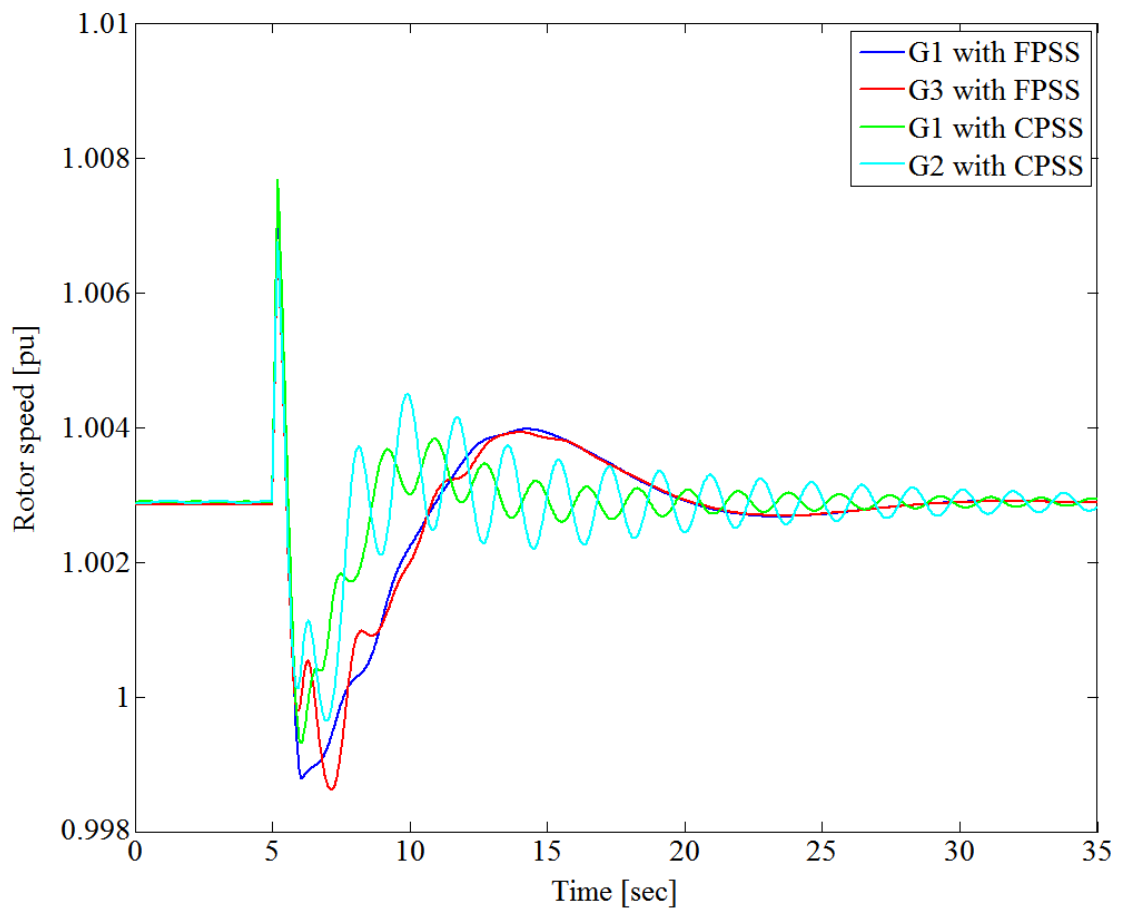


Figure 28: Response of the rotor speed of generator 1 and generator 2

Figure 28 confirms that the rotor speed with the FPSS returned back to its steady state value much earlier than with the CPSS.

From Figures 24-28, it can be deduced that the designed FPSS provides more damping to the low frequency oscillations and its dynamic performance is better compared to the CPSS.

5.4.1 System Behavior with Increase in the Load

The second scenario was to change the operating point by increasing the load at area 2.

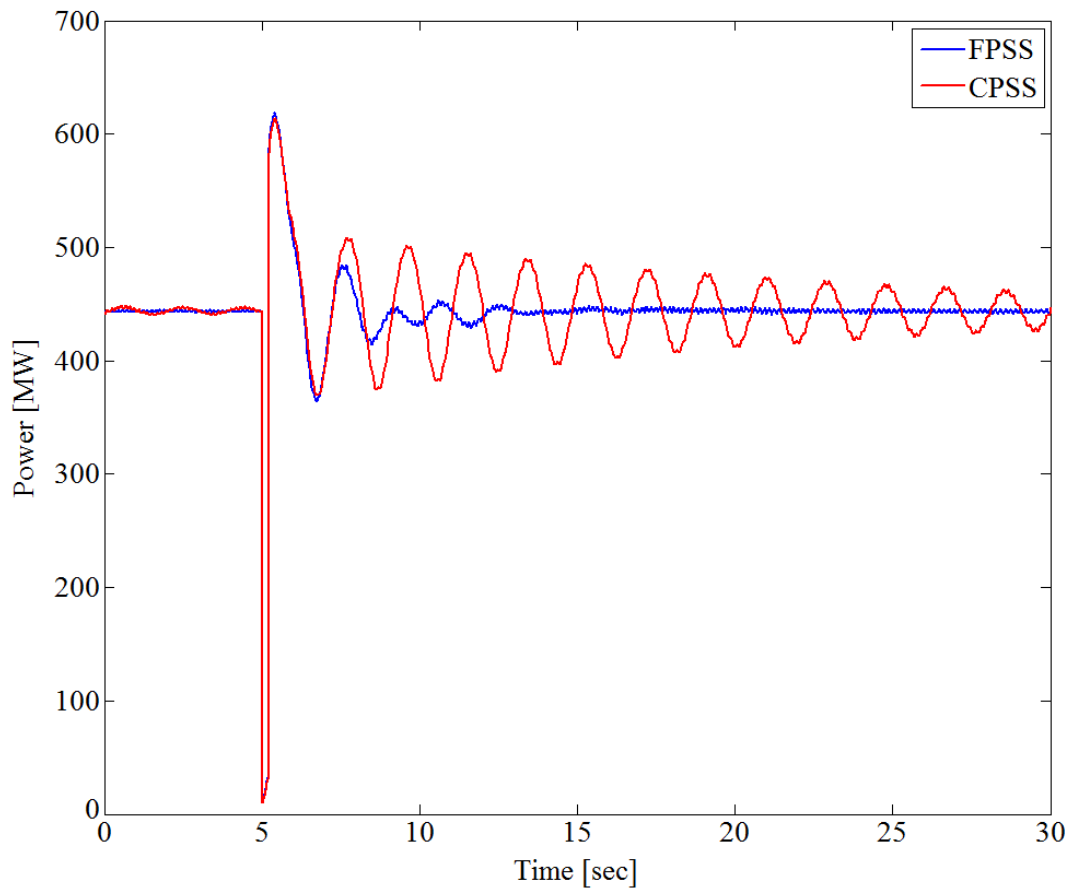


Figure 29: Response of the power exported from area 1 to area 2 with increase in the load by 5% in area 2

From Figure 29, it can be inferred that both of the FPSS and CPSS could withstand that change in the operating point (increase in the load by 5%), but when the load in area 2 was increased by 10%, the efficient performance of the FPSS in varying environment for different operating points become more obvious as shown in the Figure 30.

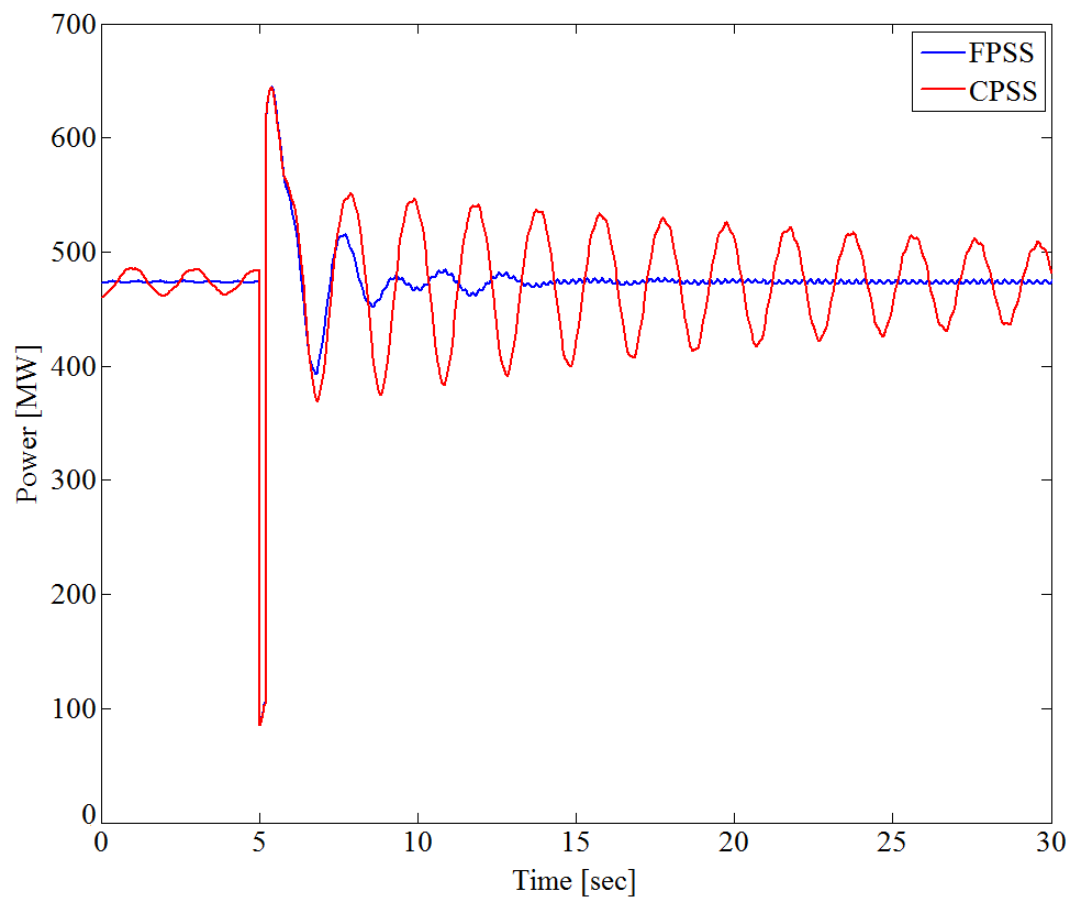


Figure 30: Response of the power exported from area 1 to area 2 with increase in the load by 10% in area 2

Compared to the Figure 24, the amplitude of the low frequency oscillations become higher with CPSS when the load increased by 10% as in Figure 28.

The next step was to increase the load in area 2 by 20% and the response is shown in Figure 31.

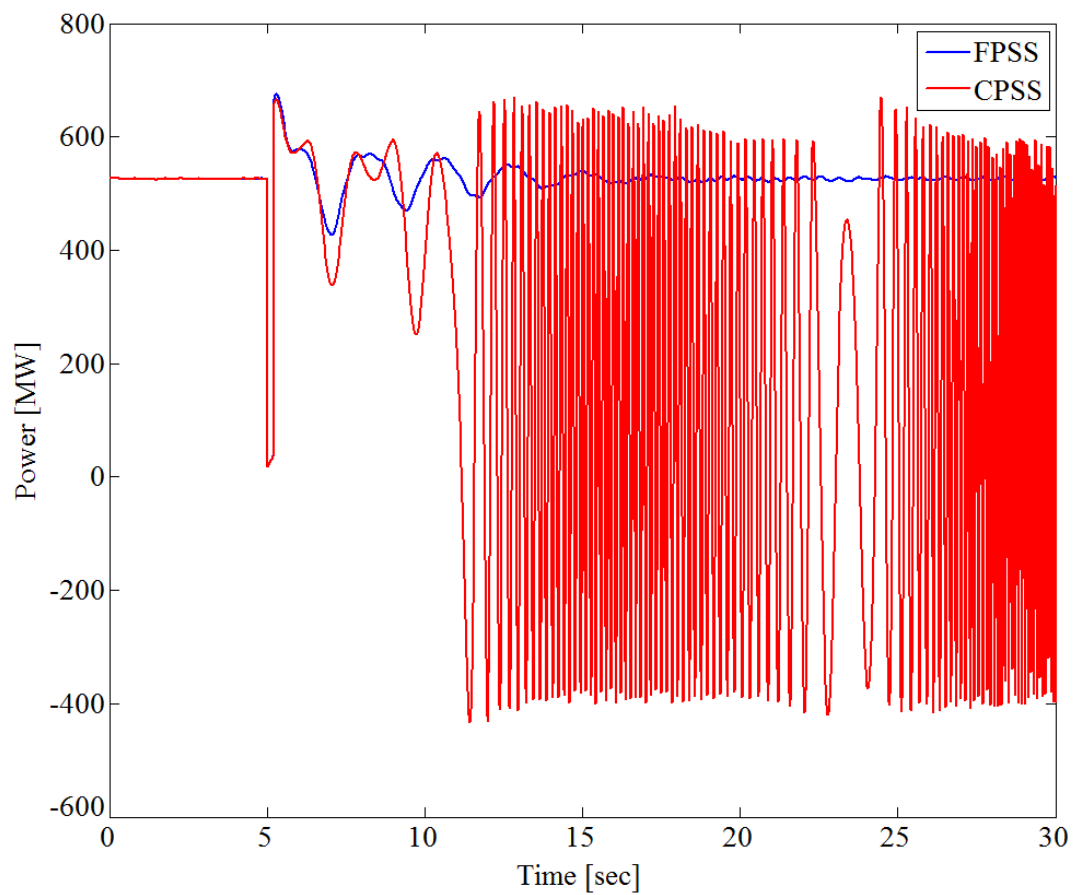


Figure 31: Response of the power exported from area 1 to area 2 with increase in the load by 20% in area 2

It is obvious that the system lost its synchronism and become unstable with the CPSS.

5.2 Summary of the Simulation

MTLAB/Simulink simulation has shown that the performance of the designed FPSS in damping the inter-area low frequency oscillations is better than the CPSS, especially when the operating point has been changed.

However, the simulation supposes that everything after the fault returns to its status before the fault which may not be true in the real life. So, the performance of the CPSS will become worst.

In comparison to what is obtained in [59], with the three-phase to ground fault, Gholipour got the response shown in Figure 32 for the power transmitted between the two areas.

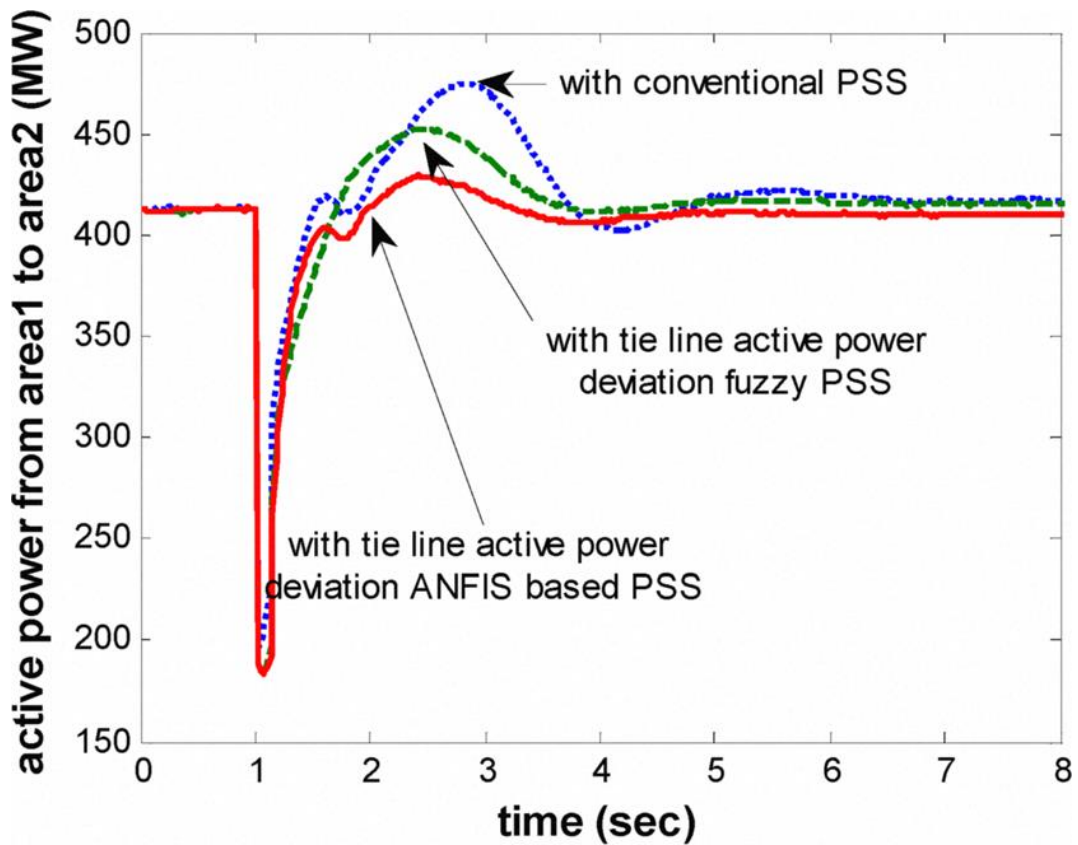


Figure 32: Response of the power transmitted from Area 1 to Area 2 [59].

As it can be inferred from Figure 32, the system become stable in about 6 sec with Gholipour proposed FPSS, while the system become stable with the proposed FPSS in this thesis in about 8 sec. The reason for the better response with Gholipour proposed FPSS may be the use of Sugeno model instead of Mamdani model as well as the use of Adaptive Neuro Fuzzy Inference System (ANFIS) in tuning the range of each membership function instead of making the range of each membership function as constant equal value, i.e. 0.66 as done in this thesis.

Chapter 6: Implementation and Experimental Results

This chapter is dedicated to show the implementation of the designed FPSS. The Experimental Results & tuning has been performed using both of Real-Time Digital Simulator (RTDS) and Phasor Measurement Unit (PMU). The Experimental setup is illustrated in Figure 33.

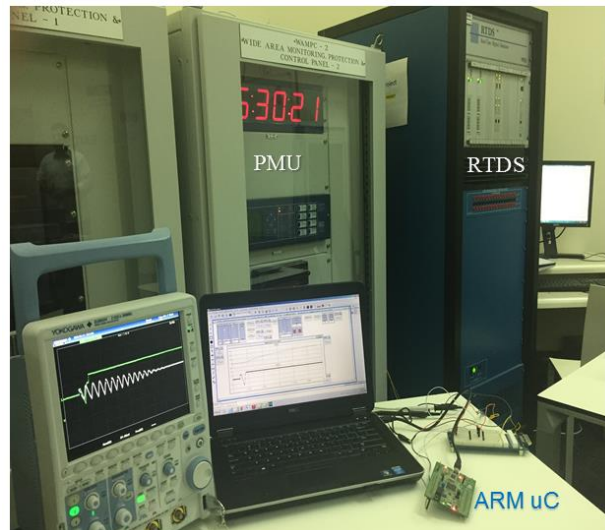


Figure 33: Experimental Setup

6.1 Implementation on SMIB

To check that the designed FPSS works, it was tested on Single Machine Infinite Bus (SMIB) first. The dynamic model of the synchronous machine is the

3rd order model which has been used in RTDS system models and the parameters of it are:

$$T'_{d0} = 8.0 \text{ sec}, X_d = 1.81 \text{ pu}, X'_d = 0.3 \text{ pu}, X_q = 1.76 \text{ pu}, H = 6.5 \text{ sec}, \omega_s = 377 \text{ rad/sec}$$

The experimental setup has been tested by applying a fault with 0.200 sec clearing time on faulted bus in SMIB system that is shown in Figure 34. The PMU is used to measure the frequency deviation (Δf) as the PMUs signal is more accurate than the conventional measurement units. (Δf) and its differentiation ($\Delta \dot{f}$) have been fed to the designed FPSS.

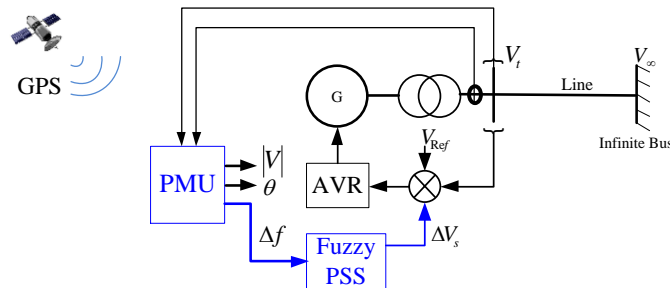


Figure 34: SMIB power system

Figures 35 and 36 show the time domain simulations of the SMIB system.

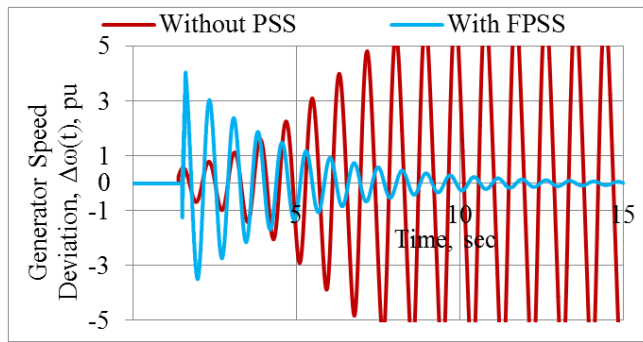


Figure 35: Response of generator speed of SMIB

From Figure 35, it can be observed that the speed deviation goes to instability without having PSS. While, with the presence of PMU based FPSS, the SMIB power system become stable.

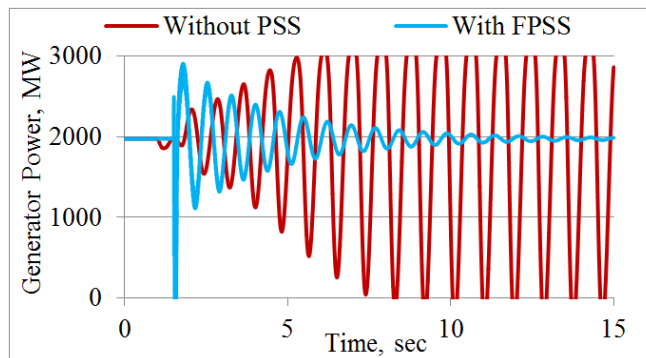


Figure 36: Response of generator output power of SMIB

The same issue with the power which strongly oscillates without PSS, but with the FPSS it become stable as in Figure 36.

The state-space model of the SMIB has been developed and the modal (eigenvalues) analysis was performed to identify the electro-mechanical oscillations mode with the presence and absence of PSS. The results of modal analysis is given in Table 8 and it is clear that the electro-mechanical oscillations mode is unstable in the absence of the PSS as the real part of the eigenvalue is positive with negative damping, $\zeta = 0.0271$, while it is stable with PSS where the real part of the eigenvalue is negative with positive damping, $\zeta = 0.0283$. The results confirm the time-domain simulations.

Table 8: Eigenvalues associated with electro-mechanical oscillation mode

Without PSS	$\lambda = + 0.1614 + j5.9503, \zeta = -0.0271, f = 0.9475$
With PSS Based on PMU	$\lambda = - 0.1548 - j5.4599, \zeta = +0.0283, f = 0.8694$

6.2 Implementation on Two-Area Power System

The two-area power system model that is shown in Figure 37 has been considered here. The parameters of the modal are the same as what is used in Chapter 5.

At each area, Phasor Measurement Unit are used to measure the frequency deviation (Δf) from which (Δf) has been derived. (Δf) and its differentiation ($\Delta \dot{f}$) have been fed to the designed FPSS.

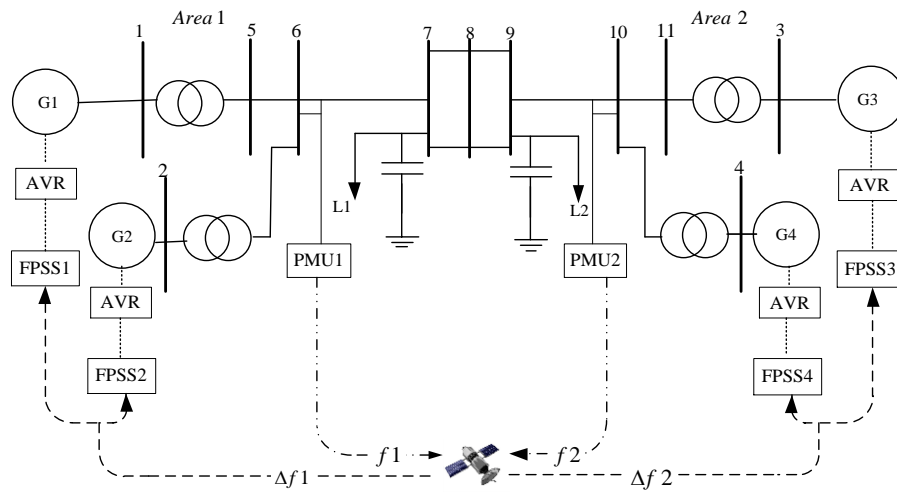


Figure 37: One-line diagram of the 4-machine 2-area power test system with PMU in each area

6.2.1 Time Response with Fault:

The experimental setup has been tested by applying a symmetrical three phase to ground (L-L-L-G) with 0.200 sec fault clearing time at bus 8 to investigate the performance of the designed FPSS.

From Figure 38, it can be observed that the voltage at the faulted bus (bus 8) goes to instability without PSS. When FPSS based on PMU signals is added to the two-area power system, it become stable.

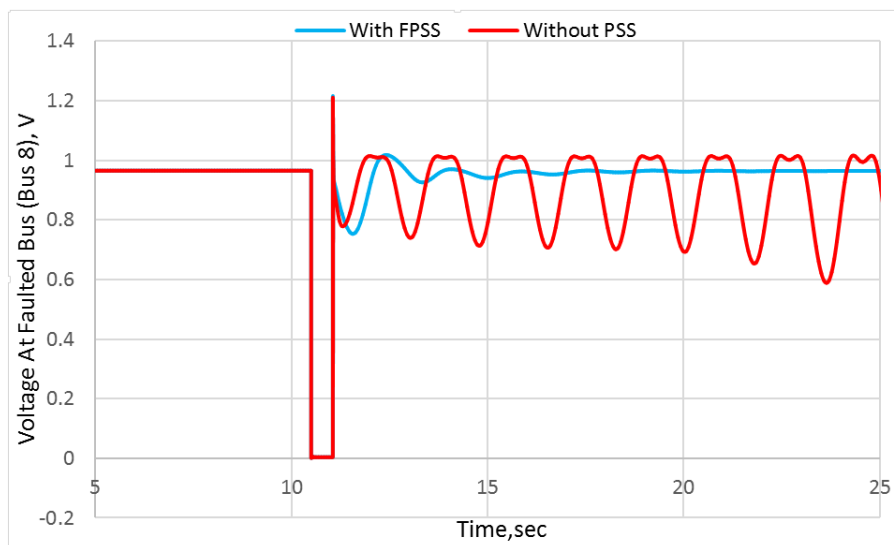


Figure 38: Response of voltage at the faulted bus

The response of the power transmitted between the two-areas under fault condition is shown in Figure 39. It can be seen from the time response that the power transferred become stable after adding FPSS.

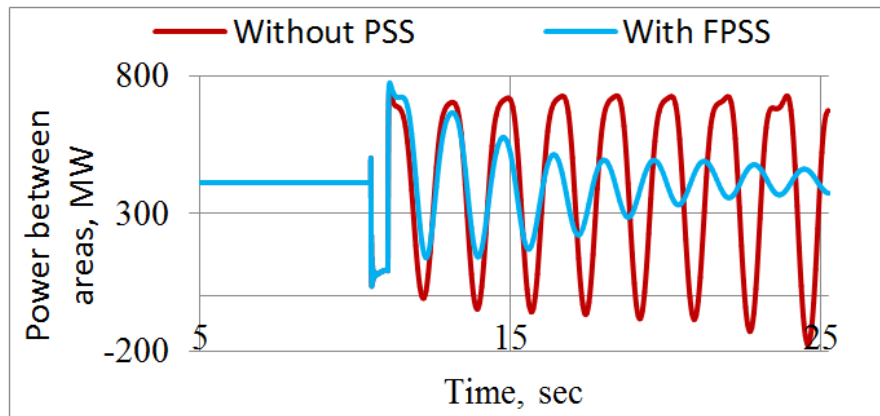


Figure 39: Response of the power exported to area 2 from area 1

From Figure 40, it can be noticed that the change in the rotor speed at the receiving end (area 2) is higher than the change at the sending end (area 1). That change happened because the average voltages of the load are decreased.

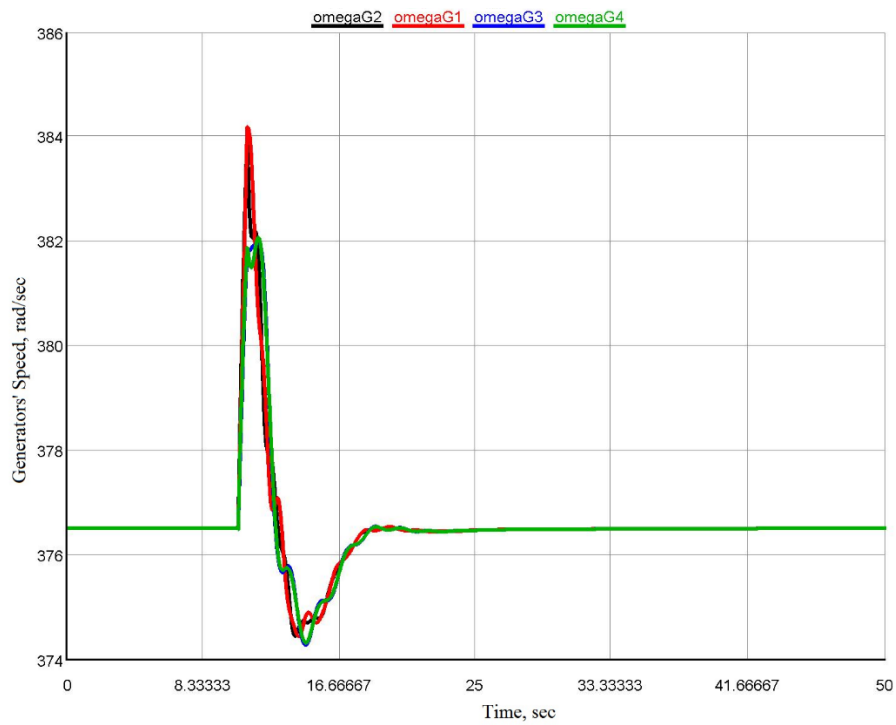


Figure 40: Response of the rotor speed for the four generators with FPSS with all generators

6.2.2 Best Location for Single FPSS

In the previous subsection, the testing scenario was with FPSS at each of the 4 generators in the two-area power system. To find the best location for a single FPSS based on PMU signals, the time responses obtained for the designed FPSS that is used in one area at a time.

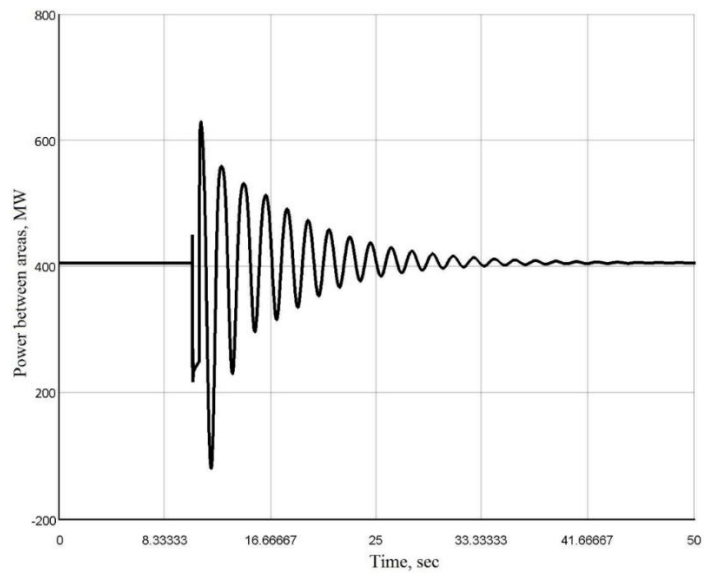


Figure 41: Response of the power exported to area 2 from area 1 with FPSS at area 1 only

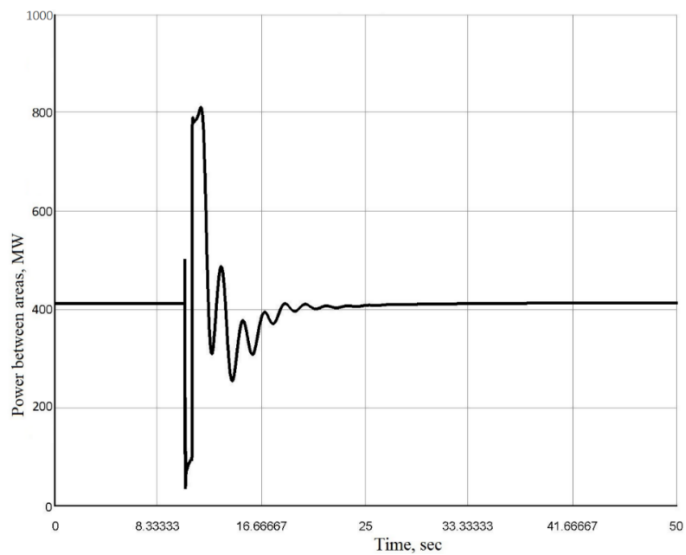


Figure 42: Response of the power exported to area 2 from area 1 with FPSS at area 2 only

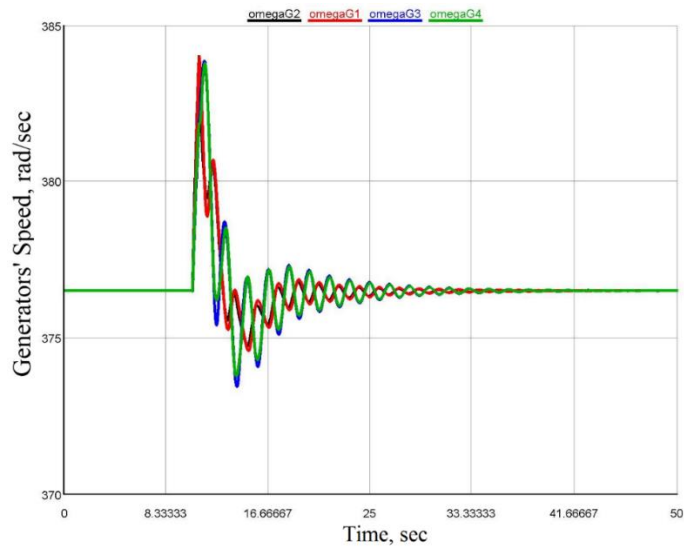


Figure 43: Response of the rotor speed for the four generators with FPSS in Area 1 only

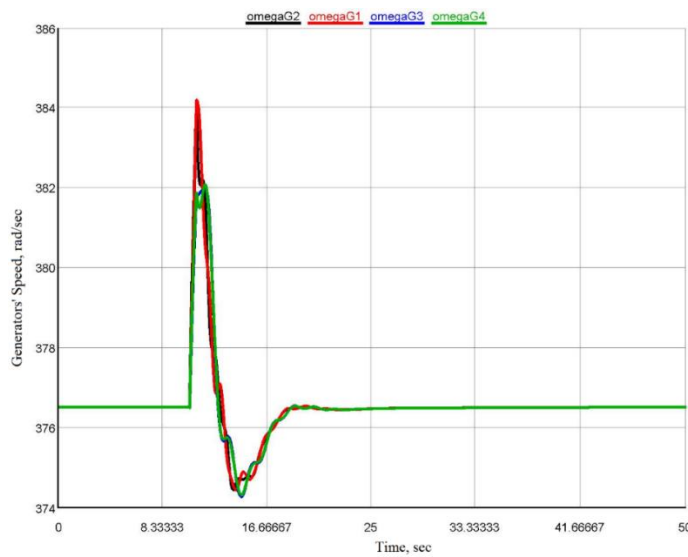


Figure 44: Response of the rotor speed for the four generators with FPSS in Area 2 only

From Figures 41-44, it can be concluded that the performance of the designed FPSS when it is added to area 2 is better than when it is added to area 1. The next step is to check the performance of the designed FPSS when added only to either generator 3 or generator 4.

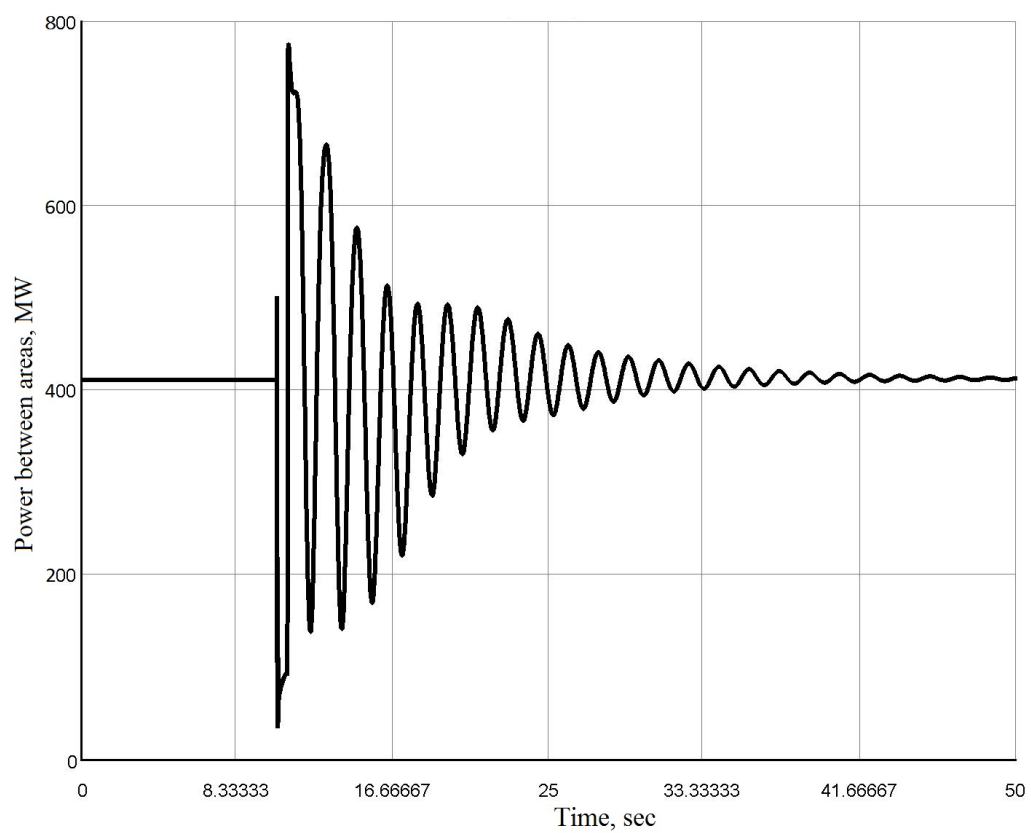


Figure 45: Response of the power exported to area 2 from area 1 with FPSS on Generator 3 only.

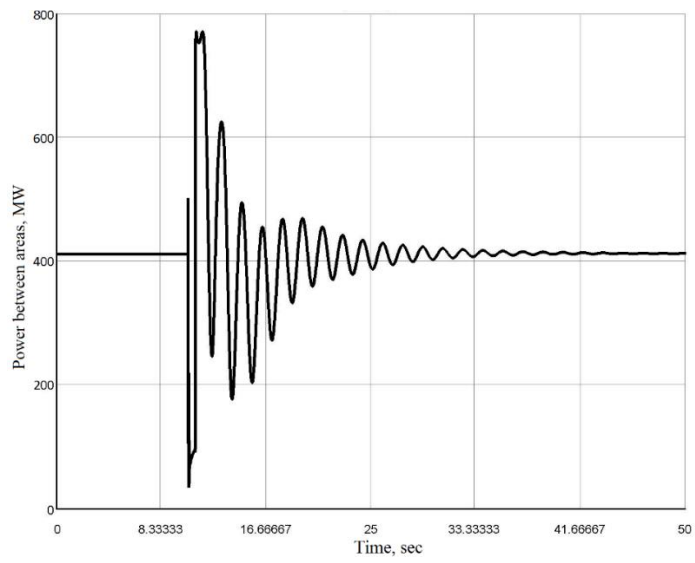


Figure 46: Response of the power exported to area 2 from area 1 with FPSS on Generator 4 only.

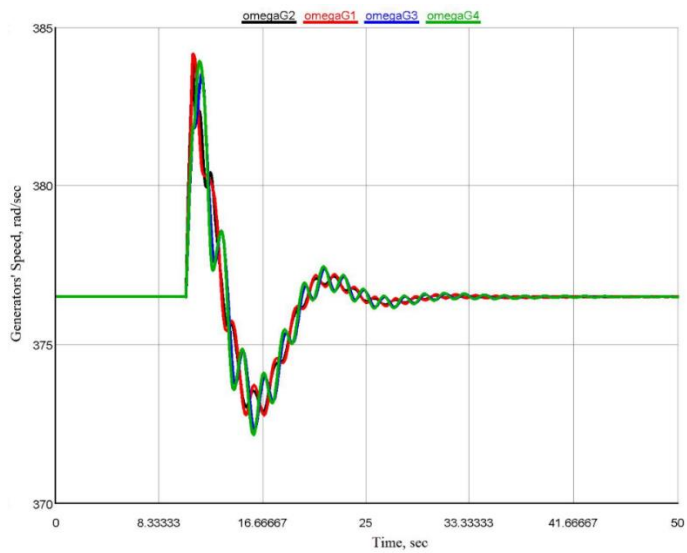


Figure 47: Response of the rotor speed for the four generators with FPSS with generator 3 only

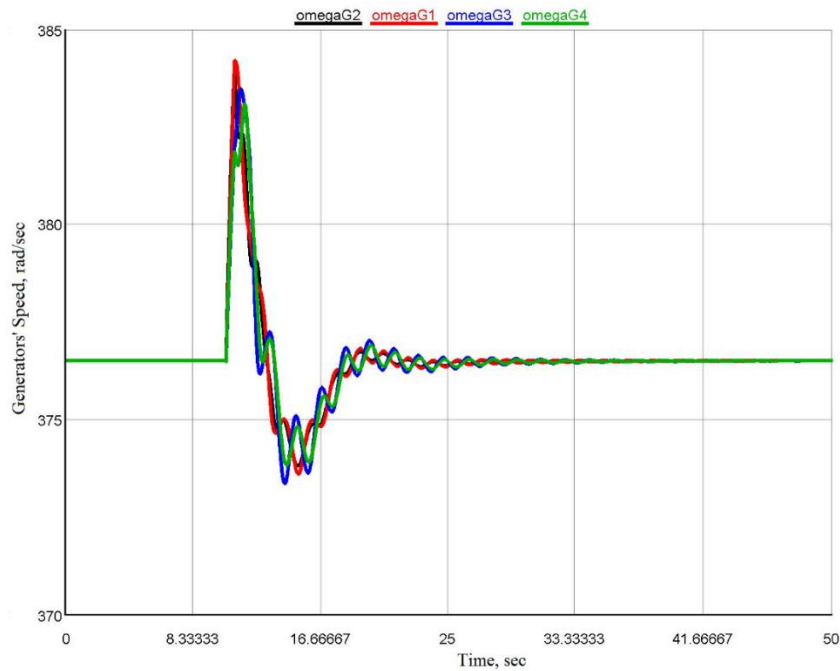


Figure 48: Response of the rotor speed for the four generators with FPSS with generator 4 only

Hence, from Figures 45-48, it can be concluded that the best location for the designed FPSS is to add it to the excitation system of the generator 4.

The state-space model of the two-area system has been developed and the modal (eigenvalues) analysis has been performed to identify the inter-area oscillation mode with and without PSS. The eigenvalues corresponding to the inter area oscillation mode are given in Table 9 and it can be seen that the oscillation is stable with the PSS as the real part of the eigenvalue is negative with positive damping, $\zeta = 0.2703$.

Table 9: Eigenvalues associated with inter-area oscillation mode

Without PSS	$\lambda_{1,2} = +0.06 \pm j3.73, \zeta = -0.0161, f = 0.5939$
With PSS Based on PMU	$\lambda_{1,2} = -1.05 \pm j3.74, \zeta = +0.2703, f = 0.5955$

Chapter 7: Conclusion and Future Work

7.1 Conclusion

In this thesis, a fuzzy logic based power system stabilizer (FPSS) has been designed. It was simulated using MATLAB/Simulink model for the two-area power system and the performance of it compared with the CPSS. While the conventional power system stabilizer can provide sufficient damping for a specific range around the point to which it is tuned, the fuzzy logic based PSS is an adaptive in nature which can stabilize the system under any operating conditions. The results of the simulation part compared with the results obtained in [59] which is slightly better in terms of less settling time. The possible reason for the better response in [59] than what is obtained in this thesis may be the use of Sugeno model with ANFIS.

Also, the designed FPSS has been implemented using ARM cortex M-4 μ -controller and tested in real time on both of the SMIB system and the two-area power system. The analog inputs to the PMUs are the measured system voltages and currents that obtained from the RTDS system model. The measured global signals of PMUs are used as the input to the real-time FPSS. The proposed FPSS enhanced effectively the damping of both local and inter-area oscillation modes and hence improved the stability of the system. The main objective of this study is to analyze the potential applications of real-time fuzzy logic PSS based on PMUs signals in the Gulf Cooperation Council (GCC) power grid as its interconnected power systems are expected to face a stability problem due to the poorly damped inter-area oscillation modes. These poorly damped oscillations are caused by

transferring large amount of power through the weak tie-lines that connected the systems in the power grid.

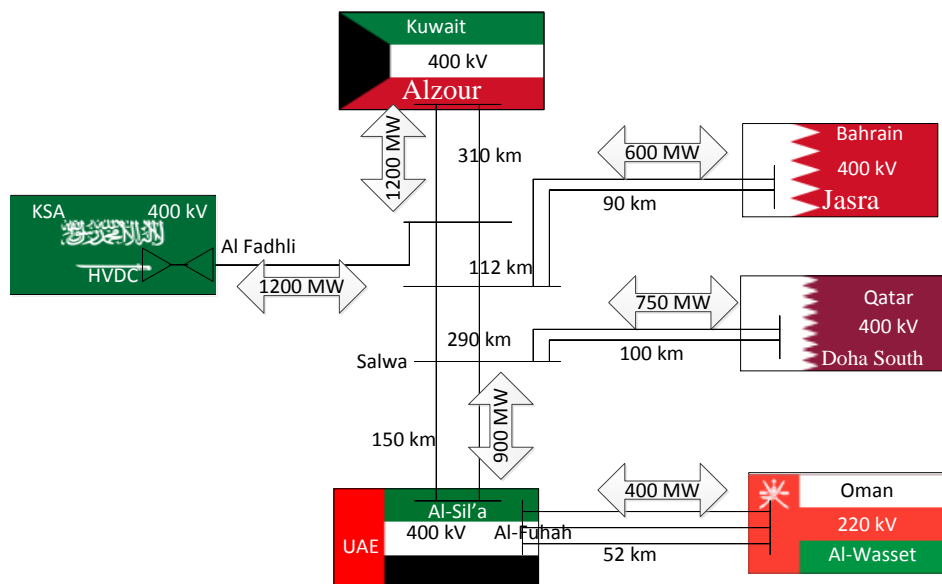


Figure 49: GCC Interconnected Power Grid [14]

7.2 Future Work

Since the range of membership function selected to be equal each one, a possible next step to slightly enhance the performance of the FPSS could be changing the ranges of the membership function using Particle Swarm Optimization to make the designed FPSS automatically tuned. Also, the performance of the FPSS will be compared using different types of the membership functions and different

input signals, especially the active tie-line power deviation. Additionally, the designed FPSS will be tested on more complex interconnected power systems models.

References

- [1] Pal, B. and Chaudhuri, B., 2005. Power system oscillations. Robust Control in Power Systems, pp.5-12.
- [2] Kundur, P., Paserba, J., Ajarapu, V., Andersson, G., Bose, A., Canizares, C., Hatziargyriou, N., Hill, D., Stankovic, A., Taylor, C. and Cutsem, T.V., 2004. Definition and classification of power system stability IEEE/CIGRE joint task force on stability terms and definitions. *Power Systems, IEEE Transactions on*, 19(3), pp.1387-1401.
- [3] Machowski, J., Bialek, J. and Bumby, J., 2011. Power system dynamics: stability and control. John Wiley & Sons.
- [4] De Marco, F.J., Martins, N. and Rezende Ferraz, J.C., 2013. An automatic method for power system stabilizers phase compensation design. *Power Systems, IEEE Transactions on*, 28(2), pp.997-1007.
- [5] Klein, M., Rogers, G.J. and Kundur, P., 1991. A fundamental study of inter-area oscillations in power systems. *IEEE Transactions on Power Systems*, 6(3), pp.914-921.
- [6] Yun, W.C. and Zhang, Z.X., 2006. Electric power grid interconnection in Northeast Asia. *Energy Policy*, 34(15), pp.2298-2309.
- [7] Smiti, A. and Eloudi, Z., 2013, June. *Soft dbscan: Improving dbscan clustering method using fuzzy set theory. In Human System Interaction (HSI), 2013 The 6th International Conference on (pp. 380-385). IEEE.*
- [8] Dobrin, C., Piuleac, C.G., Bondrea, I., Vrinceanu, N. and Florea, M., Hybride Approach Based On Genetic Algorithms And Neural Networks In Decision Making Within A Virtual Factory.

- [9] Gad, A. and Farooq, M., 2001. Application of fuzzy logic in engineering problems. In Industrial Electronics Society, 2001. IECON'01. The 27th Annual Conference of the IEEE (Vol. 3, pp. 2044-2049). IEEE.
- [10] Sathyavani, D. and Sharmila, D., International Journal of Engineering Sciences & Research Technology An Optimized Method For Finding High Utility Itemsets Using Fuzzy Tail Node Tree (FTNT).
- [11] Soh, Y.W., 2013. *Self navigating wheelchair control (obstacle avoidance) (Doctoral dissertation, UTAR)*.
- [12] A. Phadke and J. S. Thorp, "Synchronized phasor measurements and their applications," vol. 1, New York: Springer, 2008, p.81.
- [13] Deese, A.S.; Nugent, T.; Coppi, S., "A comparative study of optimal PMU placement algorithms for cost minimization," PES General Meeting | Conference & Exposition, 2014 IEEE , vol., no., pp.1,5, 27-31 July 2014.
- [14] Ajamal, A., Elthalathiny, M. and Ellithy, K., 2015, February. PSSs design based on PMUs signals to enhance the stability of inter-area oscillations of interconnected power systems. In Power and Energy Conference at Illinois (PECI), 2015 IEEE (pp. 1-5). IEEE.
- [15] Hashim, N., Hamzah, N., Latip, M.A. and Sallehuddin, A.A., 2012, February. Transient stability analysis of the IEEE 14-bus test system using dynamic computation for power systems (DCPS). In Intelligent Systems, Modelling and Simulation (ISMS), 2012 Third International Conference on (pp. 481-486). IEEE.
- [16] Kundur P. (1994). *Power System Stability and Control. McGraw-Hill*.

- [17] Snyder, A.F., Hadjsaid, N., Georges, D., Mili, L., Phadke, A.G., Faucon, O. and Vitet, S., 1998, August. Inter-area oscillation damping with power system stabilizers and synchronized phasor measurements. In *Power System Technology, 1998. Proceedings. POWERCON'98. 1998 International Conference on* (Vol. 2, pp. 790-794). IEEE.
- [18] Awed-Badeeb, O.M., 2006. Damping of electromechanical modes Using power system stabilizers (PSS) Case: electrical yemeni network. *Journal of Electrical Engineering-Bratislava-*, 57(5), p.291.
- [19] Atienza, E. and Moxley, R., 2009, October. Improving Breaker Failure Clearing Times. In *proceedings of the 36th Annual Western Protective Relay Conference, Spokane, WA.*
- [20] Naimi, D., Bouktir, T. and Salhi, A., 2013, March. Improvement of transient stability of Algerian power system network with wind farm. In *Renewable and Sustainable Energy Conference (IRSEC), 2013 International* (pp. 251-256). IEEE.
- [21] Kadriu, K., Gashi, A., Gashi, I., Hamiti, A. and Kabashi, G., 2013. Influence of dc Component during Inadvertent Operation of the High Voltage Generator Circuit Breaker during Mis-Synchronization.
- [22] Gupta, N. and Jain, S.K., 2010. Comparative analysis of fuzzy power system stabilizer using different membership functions. *International Journal of Computer and Electrical Engineering*, 2(2), p.262.
- [23] Alkhatib, H. and Duveau, J., 2013. Dynamic genetic algorithms for robust design of multimachine power system stabilizers. *International Journal of Electrical Power & Energy Systems*, 45(1), pp.242-251.

- [24]Mostafa, H.E., El-Sharkawy, M.A., Emary, A.A. and Yassin, K., 2012. Design and allocation of power system stabilizers using the particle swarm optimization technique for an interconnected power system. *International Journal of Electrical Power & Energy Systems*, 34(1), pp.57-65.
- [25]Ellithy, K., Said, S. and Kahlout, O., 2014. Design of power system stabilizers based on μ -controller for power system stability enhancement. *International Journal of Electrical Power & Energy Systems*, 63, pp.933-939.
- [26]Bevrani, H., Hiyama, T. and Bevrani, H., 2011. Robust PID based power system stabiliser: design and real-time implementation. *International Journal of Electrical Power & Energy Systems*, 33(2), pp.179-188.
- [27]Segal, R., Sharma, A. and Kothari, M.L., 2004. A self-tuning power system stabilizer based on artificial neural network. *International journal of electrical power & energy systems*, 26(6), pp.423-430.
- [28]Sumina, D., Bulić, N. and Mišković, M., 2011. Parameter tuning of power system stabilizer using eigenvalue sensitivity. *Electric power systems research*, 81(12), pp.2171-2177.
- [29]Radaideh, S.M., Nejdawi, I.M. and Mushtaha, M.H., 2012. Design of power system stabilizers using two level fuzzy and adaptive neuro-fuzzy inference systems. *International Journal of Electrical Power & Energy Systems*, 35(1), pp.47-56.
- [30]Ul Banna, H., Luna, A., Rodriguez, P., Cabrera, A., Ghorbani, H. and Ying, S., 2014, October. Performance analysis of conventional PSS and fuzzy controller for damping power system oscillations. In *Renewable Energy*

- Research and Application (ICRERA), 2014 International Conference on* (pp. 229-234). IEEE.
- [31] Gupta, R., Sambariya, D.K. and Gunjan, R., 2006, December. Fuzzy logic based robust power system stabilizer for multi-machine power system. In *Industrial Technology, 2006. ICIT 2006. IEEE International Conference on* (pp. 1037-1042). IEEE.
- [32] You, R., Eghbali, H.J. and Nehrir, M.H., 2003. An online adaptive neuro-fuzzy power system stabilizer for multimachine systems. *Power Systems, IEEE Transactions on*, 18(1), pp.128-135.
- [33] Shah, B., 2013, April. Comparative Study of Conventional and Fuzzy Based Power System Stabilizer. In *Communication Systems and Network Technologies (CSNT), 2013 International Conference on* (pp. 547-551). IEEE.
- [34] Soliman, M., Elshafei, A.L., Bendary, F. and Mansour, W., 2009. LMI static output-feedback design of fuzzy power system stabilizers. *Expert Systems with Applications*, 36(3), pp.6817-6825.
- [35] Watson, W. and Manchur, G., 1973. Experience with supplementary damping signals for generator static excitation systems. *Power Apparatus and Systems, IEEE Transactions on*, (1), pp.199-203.
- [36] Umrao, R. and Chaturvedi, D.K., 2013. A novel fuzzy control approach for load frequency control. In *Recent Advancements in System Modelling Applications* (pp. 239-247). Springer India.

- [37] Hussein, T., Saad, M.S., Elshafei, A.L. and Bahgat, A., 2010. Damping inter-area modes of oscillation using an adaptive fuzzy power system stabilizer. *Electric Power Systems Research*, 80(12), pp.1428-1436.
- [38] Ramirez-Gonzalez, M. and Malik, O.P., 2010. Self-tuned power system stabilizer based on a simple fuzzy logic controller. *Electric Power Components and Systems*, 38(4), pp.407-423.
- [39] El-Metwally, K.A., 2008, July. Power System Stabilization Using Swarm Tuned Fuzzy Controller. In *World Congress* (Vol. 17, No. 1, pp. 11106-11111).
- [40] Sambariya, D.K. and Prasad, R., 2013, January. Robust power system stabilizer design for single machine infinite bus system with different membership functions for fuzzy logic controller. In *Intelligent Systems and Control (ISCO), 2013 7th International Conference on* (pp. 13-19). IEEE.
- [41] Zhao, J. and Bose, B.K., 2002, November. Evaluation of membership functions for fuzzy logic controlled induction motor drive. In *IECON 02 [Industrial Electronics Society, IEEE 2002 28th Annual Conference of the]* (Vol. 1, pp. 229-234). IEEE.
- [42] Weckesser, T., Jóhannsson, H. and Ostergaard, J., 2013, August. Impact of model detail of synchronous machines on real-time transient stability assessment. In *Bulk Power System Dynamics and Control-IX Optimization, Security and Control of the Emerging Power Grid (IREP), 2013 IREP Symposium* (pp. 1-9). IEEE.
- [43] Sauer, P.W. and Pai, M.A., 1998. Power system dynamics and stability. *Urbana*.

- [44] B. Bayati Chaloshitori, S. Hoghoughi Isfahani, N.R. Abjadi, 2011. "A Comparison between a Conventional Power System Stabilizer (PSS) and Novel PSS Based on Feedback Linearization Technique", *Journal of Basic and Applied Scientific Research*, 1(11) pp.1920- 1929.
- [45] Jerković, V., Miklošević, K. and Željko, Š., 2010, January. Excitation system models of synchronous generator. In *SiP 2010 28th International Conference Science in Practice*.
- [46] Lee, D.C., 2005. IEEE recommended practice for excitation system models for power system stability studies (IEEE Std 421.5-2005). Energy Development and Power Generating Committee of the Power Engineering Society.
- [47] El-Hawary, Mohamed E. (2008). *Introduction to Electrical Power Systems*. John Wiley & Sons. ch-5 pp.129- 130.
- [48] Karady, George G., Grisby, Leonard L. *Transmission System," The electric power engineering handbook*. CRC press, 2012. ch-4.
- [49] Chakrabarti, S., 2009. Static load modelling and voltage stability indices. *International Journal of Power and Energy Systems*, 29(3), pp.200-205.
- [50] Lipo, T.A., 2012. *Analysis of synchronous machines*. CRC Press.
- [51] Arizadayana, Z., Irwanto, M., Fazliana, F. and Syafawati, A.N., 2014, March. Improvement of dynamic power system stability by installing UPFC based on Fuzzy Logic Power System Stabilizer (FLPSS). In *Power Engineering and Optimization Conference (PEOCO), 2014 IEEE 8th International* (pp. 188-193). IEEE.

- [52]Rout, K.C., 2011. *Dynamic Stability Enhancement of Power System Using Fuzzy Logic Based Power System Stabilizer* (Doctoral dissertation).
- [53]Zhao, P., Gao, Y., Zhou, H. and Turng, L.S., 2013. Noniterative Optimization Methods. *Computer Modeling for Injection Molding: Simulation, Optimization, and Control*, pp.255-282.
- [54]Kundur P. (1994). *Power System Stability and Control*. McGraw-Hill, pp : 710-830
- [55]Demello, F.P. and Concordia, C., 1969. Concepts of synchronous machine stability as affected by excitation control. *IEEE Transactions on power apparatus and systems*, 88(4), pp.316-329.
- [56]Patel, H.D. and Majmudar, C., 2011, December. Fuzzy logic application to single machine power system stabilizer. In *Engineering (NUiCONE), 2011 Nirma University International Conference on* (pp. 1-6). IEEE.
- [57]Khezri, R. and Bevrani, H., 2015. Voltage performance enhancement of DFIG-based wind farms integrated in large-scale power systems: Coordinated AVR and PSS. *International Journal of Electrical Power & Energy Systems*, 73, pp.400-410.
- [58]Dhillon, S.S., Lather, J.S. and Marwaha, S., 2015. Multi Area Load Frequency Control Using Particle Swarm Optimization and Fuzzy Rules. *Procedia Computer Science*, 57, pp.460-472.
- [59]Gholipour, A., Lesani, H. and Zadeh, M.K., 2009, December. Performance of a ANFIS based PSS with tie line active power deviation feedback. In *Power Electronics and Intelligent Transportation System (PEITS), 2009 2nd International Conference on* (Vol. 2, pp. 267-273). IEEE.

- [60] Singh, B., Sharma, N.K., Tiwari, A.N., Verma, K.S. and Singh, S.N., 2011. Applications of phasor measurement units (PMUs) in electric power system networks incorporated with FACTS controllers. *International Journal of Engineering, Science and Technology*, 3(3).
- [61] Chakrabarti, S., Kyriakides, E., Ledwich, G. and Ghosh, A., 2010. Inclusion of PMU current phasor measurements in a power system state estimator. *Generation, Transmission & Distribution, IET*, 4(10), pp.1104-1115.

Appendix A: Papers and Posters

Title of the Poster/Paper	Journal/Conference	Country	Status
Design of Real-Time Fuzzy Logic PSS Based on PMUs for Damping Low Frequency Oscillations	IEEE PES GM 2015 Conference	USA	Presented
Design of Fuzzy PSSs Based on PMUs Global Signals for Damping Low Frequency Oscillations of GCC Power Grids	11 th GCC – CIGRE	Qatar	Under Review
Design of Fuzzy PSSs Based on PMUs Global Signals for Damping Low Frequency Oscillations of Smart Power Systems	ASME Power 2016	USA	Reviewed & accepted
Design of Fuzzy PSSs Based on PMUs Global Signals for Damping Low Frequency Oscillations of Smart Power Systems	Ain Shams Engineering Journal	Egypt	Under Review

Appendix B: RTDS Model

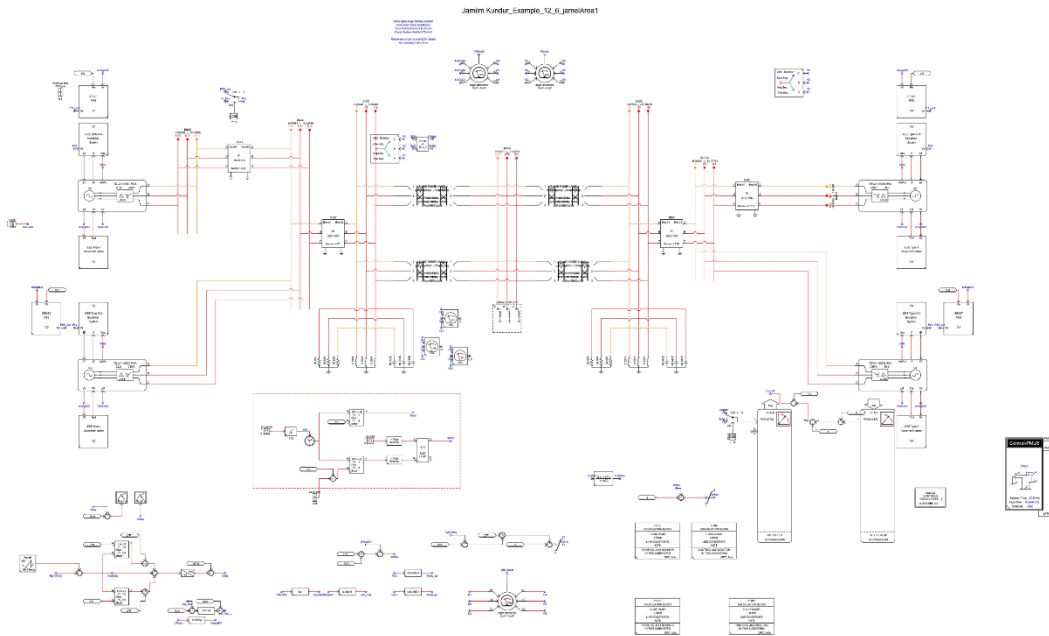


Figure 50: Two-area power system model in RTDS

Appendix C: MATLAB Code used for FPSS

Table 10: MATLAB code for inserting FIS file in Fuzzy Logic Controller

```
clear

Fuzzy_matlab_working = readfis('Fuzzy_model_matlab');

model_name='PSS';

% load_system(model_name)
% result=zeros(10);
% ii=1;
% PPP=[];
% index=1;
% h=figure;
%
ss='D:\Users\jamil\\Desktop\Master\Graduate\Thesis;
%
% for i=10:1:10 % the input
%     for j=21:1:50 % the output
%         result(ii+j-1,3)=new_func2([j i]);
%         result(ii+j-1,1)=i; % input scal
%         result(ii+j-1,2)=j; % output scal
%         PPP(:,index)=PP;
%         plot(PPP(:,index))
%         s=sprintf('input scale %d output scale
%d',i,j);
%         title(s)
%         saveas(h,[ss,s],'jpg')
%
%         index=index+1;
%     end
%
% ii=ii+j-1+1;
% %P=sum((P(:)-400).^2)/length(P);
% i
% j
%
% end
```

Appendix D: MATLAB code for Finding Eigenvalues

Table 11: MATLAB code for Finding Eigenvalues

```
f=60;
KA=100;TA=0.1;K1=0.9831;K2=1.0923;K3=0.3864;K4=1.4746
;K5=-0.1103;
K6=0.4477;Td0=5;H=6;kpss=10; T1=0.154; T2=0.033;
D=0;
Ws=2*pi*f;

A=[ -1/(K3*Td0)  -K4/Td0      0      1/Td0  0;
      0          0          Ws      0      0;
      -K2/(2*H)  -K1/(2*H)  -D*Ws/(2*H)  0      0;
      -KA*K6/TA  -KA*K5/TA    0          -1/TA  KA/TA;
      (-kpss*K2*T1)/(2*H*T2)  (-kpss*K1*T1)/(2*H*T2)
      ((-D*kpss*T1)/(2*H*T2))/(kpss/T2)  0  -1/T2];

B = [0; 0; 0; KA/TA; 0];
C = [0 0 1 0 0];
D = [0];

[R,E]=eig(A);
L=inv(R);
L=L';
E
eig(A)
```

Appendix E: ARM μ -Controller Code

Table 12: C code for programming FPSS on μ -Controller

```
#include "ser_functions.c"
#include "fuzzy_functions.c"
#include "DAC.c"

void main() {

int adc_value;
float BP,MP,SP,Z,SN,MN,BN;
float E_BP,E_MP,E_SP,E_Z,E_SN,E_MN,E_BN;
float DE_BP,DE_MP,DE_SP,DE_Z,DE_SN,DE_MN,DE_BN;
float err,derr,ERR_sc,DERR_sc,output,output_sc,y,his_err;
int input_reading, count,i,xx;

unsigned long xxx;
//uint16_t xxx=0;
//uint32_t config;

    GPIO_Digital_Output(&GPIOA_BASE, _GPIO_PINMASK_ALL); // Set
PORTA as digital output
    GPIO_Digital_Output(&GPIOB_BASE, _GPIO_PINMASK_ALL); // Set
PORTB as digital output
    GPIO_Digital_Output(&GPIOC_BASE, _GPIO_PINMASK_ALL); // Set
PORTC as digital output
    GPIO_Digital_Output(&GPIOD_BASE, _GPIO_PINMASK_ALL); // Set
PORTD as digital output
    GPIO_Digital_Output(&GPIOE_BASE, _GPIO_PINMASK_ALL); // Set
PORTE as digital output
    GPIO_Digital_Output(&GPIOD_BASE, _GPIO_PINMASK_12); // Set
PORTD as digital output
    GPIO_Digital_Output(&GPIOD_BASE, _GPIO_PINMASK_13); // Set
PORTD as digital output
    GPIO_Digital_Output(&GPIOD_BASE, _GPIO_PINMASK_14); // Set
PORTD as digital output
    GPIO_Digital_Output(&GPIOD_BASE, _GPIO_PINMASK_15); // Set
PORTD as digital output

    ADC_Set_Input_Channel(_ADC_CHANNEL_10); // Set ADC channel 10 as
an analog input
```

```

ADC1_Init();           // Initialize ADC module
dac1_init(_DAC_CH1_ENABLE);
    output_sc=0.3      ;
    ERR_sc=10; //30
    DERR_sc=5;
    count =0;

i=0;
his_err=0;
xxx=0;

while(1)
{
//    GPIOA_ODR = ADC1_Read(10);    // ADC pin is PC0

    err=convert_AD(ADC1_Read(10));
//    err=ADC1_Read(10);

    //derr=d_error_val[i];
    derr=err-his_err;

    err=err/err_sc;
    derr=derr/derr_sc;

    fuzzification(err,&E_BN,&E_MN,&E_SN,&E_Z,&E_SP,&E_MP,&E_BP );

    fuzzification(derr,&DE_BN,&DE_MN,&DE_SN,&DE_Z,&DE_SP,&DE_MP,
    &DE_BP );

    rulebase(E_BP,E_MP,E_SP,E_Z,E_SN,E_MN,E_BN,DE_BP,DE_MP,DE_SP,
    DE_Z,DE_SN,DE_MN,DE_BN,&BP,&MP,&SP,&Z,&SN,&MN,&BN);
    defuzzification(BN,MN,SN,Z,SP,MP,BP);
    output= defuzzification(BN,MN,SN,Z,SP,MP,BP) * output_sc;
//    output = limiter(output,-0.2,0.2);

//output =0.2;
//while (1)
//{
//    output=err*0.08;

    if (output>= 0.2) output =0.2;
    else if (output<= -0.2) output=-0.2;

    y=4.756666667*(output+0.3)+0.051;
    y=y/0.000696533;

```

```
        xx=y;
        DAC1_Ch1_Output(xx); // DAC pin is PA4
//      delay_ms(2000);
//      if (output ==0.2) output=-.3;
//      if (output ==-0.2) output=.3;

// }
//      DAC1_Ch1_Output(ADC1_Read(10));
//i++;
his_err=err;

GPIOA_ODR.b6=~GPIOA_ODR.b6;

//if (i>500) i=0;
}
}
```
